Mutant Plasticity Related Gene 1 (*PRG1*) acts as a potential modifier in *SCN1A* related epilepsy

Ellen Knierim,[1,2*] Johannes Vogt,[3*] Michael Kintscher,[4,12*] Alexey Ponomarenko,[5,6] Jan Baumgart,[4] Prateep Beed,[4] Tatiana Korotkova,[5,6] Thorsten Trimbuch,[4] Axel Panzer,[7] Ulrich Stephani,[8] Andrew Escayg,[9] Holger Lerche,[10] Robert Nitsch,[3,§] Dietmar Schmitz;[4,5,12,§] Markus Schuelke[1,2,5§]

** these authors contributed equally*
§ these authors jointly directed the work

Charité–Universitätsmedizin Berlin, corporate member of Freie Universität Berlin, Humboldt-Universität zu Berlin, and Berlin Institute of Health (BIH); [1] Neurocure Clinical Research Center (NCRC), [2] Department of Neuropediatrics, [4] Neuroscience Research Center (NWFZ), [5] Cluster of Excellence NeuroCure, [11] Bernstein Center for Computational Neuroscience, Germany; Berlin 10117, Germany.

[3] Institute for Microanatomy and Neurobiology, University Medical Center, Mainz 55131, Germany.

[6] Leibniz-Institut für Molekulare Pharmakologie (FMP), Berlin 13125, Germany.

[7] Epilepsy Center / Pediatric Neurology, DRK Kliniken-Westend, Berlin 14050, Germany.

[8] Medical Center of Schleswig-Holstein, Campus Kiel, Kiel 24118, Germany.

[9] Department of Human Genetics, Emory University, Atlanta, GA 30322, USA

[10] Department of Neurology and Epileptology, Hertie Institute for Clinical Brain Research, Tübingen 72076, Germany

[12] present address: Laboratory of Synaptic Mechanisms, Brain-Mind Institute, School of Life Sciences, École Polytechnique Fédérale de Lausanne, Lausanne 1015, Switzerland

Running title: PRG1 as modifier in epilepsy

Counts

Character count:	33,876 spaces
Title length:	94 spaces
Running title:	27 spaces
Abstract:	174 words

KEYWORDS: *PRG1, PLPPR4, SCN1A*, genetic modifier, West syndrome.

Corresponding authors:

Prof. Markus Schuelke, MD, Department of Neuropediatrics, Charité—Universitätsmedizin Berlin, Augustenburger Platz 1, D-13353 Berlin, Germany, Email: markus.schuelke@charite.de, Phone: +49.30.4505.66112 (questions regarding the clinical phenotype and molecular genetics), or

Prof. Dietmar Schmitz, **PhD,** Neuroscience Research Center NWFZ, Charité-Universitätsmedizin Berlin, Charitéplatz 1, D-10117 Berlin, Germany, Email: di-

etmar.schmitz@charite.de, Phone: +49.30.4505.39054 (questions regarding electrophysiology), or

PD Dr. Johannes Vogt, MD, Institute for Microanatomy and Neurobiology, University Medical Center, Mainz, Germany, Email: johannes.vogt@unimedizin-mainz.de, Phone: +49.6131.178091 (questions regarding neuroanatomy or epilepsy models)

ellen.knierim@charite.de; johannes.vogt@unimedizin-mainz.de; michael.kintscher@epfl.ch; ponomarenko@fmp-berlin.de; jan.baumgart@unimedizin-mainz.de; prateep.beed@charite.de; korotkova@fmp-berlin.de; thorsten.trimbuch@charite.de; a.panzer@drk-kliniken-berlin.de; stephani@pedneuro.uni-kiel.de; aescayg@emory.edu; holger.lerche@uni-tuebingen.de; nitschr@uni-muenster.de; dietmar.schmitz@charite.de; markus.schuelke@charite.de

ABSTRACT

Plasticity related gene 1 encodes a cerebral neuron-specific synaptic transmembrane protein that modulates hippocampal excitatory transmission on glutamatergic neurons. In mice, homozygous Prg1-deficiency results in juvenile epilepsy. Screening a cohort of 18 patients with infantile spasms (West syndrome), we identified one patient with a heterozygous mutation in the highly conserved third extracellular phosphatase domain (p.T299S). The functional relevance of this mutation was verified by *in-utero* electroporation of a mutant *Prg1* construct into neurons of *Prg1*-knockout embryos, and the subsequent inability of hippocampal neurons to rescue the knockout phenotype on the single cell level. Whole exome sequencing revealed the index patient to additionally harbor a novel heterozygous *SCN1A* variant (p.N541S) that was inherited from her healthy mother. Only the affected child carried both heterozygous *PRG1* and *SCN1A* mutations. The aggravating effect of *Prg1*-haploinsufficiency on the epileptic phenotype was verified using the kainate-model of epilepsy. Double heterozygous $Prg1^{-/+}|Scn1a^{wt/p.R1648H}$ mice exhibited higher seizure susceptibility than either wildtype, $Prg1^{-/+}$, or $Scn1a^{wt/p.R1648H}$ littermates. Our study provides evidence that *PRG1*-mutations have a potential modifying influence on *SCN1A*-related epilepsy in humans.

INTRODUCTION

Epilepsy is one of the most common neurological disorders in humans, which across North America and Europe affects approximately five people in every 1000 (Banerjee *et al*, 2009). More than 350 epilepsy-associated genes have been described in the literature. Most of them play an important role in neuronal excitability, cortical development, or synaptic transmission (Noebels, 2017). The first discovered disease genes to be linked to epilepsy in humans and mice were all subunits of voltage- and ligand-gated ion channels. Mutations in these genes currently constitute approximately one third of nearly 150 monogenic seizure disorders (Noebels, 2017), affecting either voltage-gated [*SCN1A* (Escayg *et al*, 2000), *KCNQ2* (Singh *et al*, 1998)] or ligand-gated ion channels [*CHRNA4* (Steinlein *et al*, 1995), *GABRG2* (Baulac *et al*, 2001; Wallace *et al*, 2001)]. The concept of "channelopathy" implies that dysfunction of neuronal ion channels might lead to altered ion currents and destabilization of the membrane potential, potentially leading to increased epileptic network activity.

Mutations in *SCN1A* mainly cause two epilepsy syndromes, **(i)** a severe form of epilepsy characterized by fever-associated and afebrile seizures, called "Dravet syndrome" (Depienne *et al*, 2010) and **(ii)** a milder dominant familial epilepsy syndrome, called "Genetic Epilepsy with Febrile Seizures Plus" (GEFS+) (Escayg & Goldin, 2010). The severity of GEFS+ spans a broad phenotypical spectrum ranging from healthy carriers to simple febrile seizures, febrile seizures plus, and sometimes severe forms of epilepsy. On rare occasions *SCN1A* mutations may cause "Myoclonic-astatic epilepsy", "Infantile spasms" (West syndrome), or Familial Hemiplegic Migraine (FHM) (Dichgans *et al*, 2005; Oyrer *et al*, 2018).

The genetic background, e.g. the interplay of genes jointly contributing to a biologic function such as synthesizing a protein or establishing a neuronal network, may have a profound influence on the penetrance and severity of symptoms of genetic disorders such as epilepsy. Partially, these phenomena can be modeled in mouse strains with different seizure susceptibilities. As an example, the seizure phenotype of *Scn1a* dysfunction heavily depends on the genetic background, e.g. the same *Scn1a* mutation on the 129/SvJ background results in a much milder seizure phenotype than if expressed on the C57BL/6 background (Yu *et al*, 2006). Secondly, alleles that cause mild or no phenotypes in isolation may result in more severe epilepsy when combined, as demonstrated in double mutant mice carrying the $Scn2a^{Q54}$ transgene together with either heterozygous $Kcnq2^{p.V182M}$ or $Kcnq2^{del}$ (*Szt1*) alleles

(Kearney *et al*, 2006). Even though the importance of various genetic factors is evident in theory, they are mostly unknown.

In Dravet syndrome, a modifying effector has been suggested that may explain the variable expressivity and penetrance of epilepsy in patients with sodium channel mutations (Singh *et al*, 2009). Different modifier genes in neural hyperexcitability pathways have been demonstrated in experimental models, e.g. comprising mutations in subunits of voltage- or ligand gated ion channels (Calhoun *et al*, 2017; Frankel *et al*, 2014). Others like the Tau protein play a general role in regulating intrinsic neuronal network hyperexcitability, and deletion of its coding gene suppresses seizures and sudden unexpected death (SUDEP) in different mouse models (Holth *et al*, 2013; Gheyara *et al*, 2014).

Beyond epileptic encephalopathies that are caused by ion channel dysfunction, epilepsy is also caused by mutations in genes involved in pathways regulating synaptic transmission (Appenzeller *et al*, 2014), especially through impairment of genes that are involved in pathways of synaptic inhibitory transmission from early development through maturation of adult GABA neurotransmission (Noebels, 2015).

Here we show that one such pathway is connected with the Plasticity Related Gene 1 (*PRG1*, syn. *PLPPR4* MIM*607813). This cerebral neuron-specific membrane protein is related to lipid-phosphate phosphatases (LPP) and is highly conserved in vertebrates. PRG1 is located at the postsynaptic density of excitatory synapses of glutamatergic cortical neurons. Postsynaptic PRG1 controls lysophosphatidic acid (LPA) signaling at glutamatergic synapses *via* presynaptic LPA2 receptors (Trimbuch *et al*, 2009) thereby reducing glutamate release probability and regulating cortical excitability from early postnatal stages (Vogt *et al*, 2017). PRG1 also affects spine density and synaptic plasticity in a cell-autonomous fashion *via* activation of the protein phosphatase 2A (PP2A)/ITGB1 (Liu *et al*, 2016, 1). To test the contribution of PRG1-deficiency to the pathophysiology of epilepsy, we investigated seizure activity in genetically modified mice after kainate application, screened human patients with West syndrome for mutations in *PRG1*, and functionally validated a mutation by *ex vivo* electrophysiology recordings in an *in-utero* electroporation model.

RESULTS

PATIENT STUDIES

Case history

The female patient (**Fig. 1A**, III:2) is the second child of non-consanguineous Caucasian parents. She was born at term and developed normally until the age of 6 months, when she exhibited clusters of flexion spasms and developmental regression. The EEG showed hypsarrhythmia suggestive of West syndrome. Cranial MRI and metabolic testing for increased excretion of organic acids or amino acids were normal. Seizures stopped under treatment with sulthiame. The elder brother (III:1) and both parents (II:6, II:7) are healthy. Despite her initial developmental delay, once her seizures were controlled she progressed normally and was able to achieve age-appropriate milestones later in life. Following termination of AED treatment at 2 years of age no further seizures occurred.

Genetic screening revealed a combined heterozygous mutation in the *PRG1* and the *SCN1A* gene

We analyzed the entire coding and flanking intronic sequences of *PRG1* in a cohort of 18 unrelated patients with idiopathic infantile seizures. In patient III:2 we identified a heterozygous missense mutation [chr1:99.767.383C>G (hg19), c.896C>G, p.T299S, NM_014839] in exon 6 (**Fig. 1B, C**). The mutation is located in the third extracellular domain (**Fig. 1E**), which is evolutionary conserved in mammals and birds as well as in other LPP protein-family members (**Fig. 1D**). The c.896C>G variant was absent in 400 alleles of normal controls from Middle Europe as well as in the individuals of the 1000 genome and 5000 exome projects. It was found once in heterozygous state in one individual from Europe (Non-Finnish) amongst 245,604 alleles from the gnomAD database (http://gnomad.broadinstitute.org | accessed March 2018) (Lek *et al*, 2016). The heterozygous p.T299S variant, predicted to be 'disease causing' by MutationTaster2 (Schwarz *et al*, 2014) with a probability of P=0.983, had been inherited from her clinically unaffected father (II:7) letting us assume that the *PRG* variant might be a modifying factor of a preexisting mutation on another gene. Hence we investigated this possibility and screened for other epileptogenic mutations in patient III:2 by Whole-Exome Sequencing (WES).

WES revealed a second heterozygous missense variant [chr2:166.901.593T>C (hg19) c.1622A>G, p.N541S, NM_006920] in the *SCN1A* gene. The variant amino acid position is located in a sequence motif that is highly conserved in vertebrates (**Fig. 1D**) and was not

listed either as a polymorphism or pathogenic variant in the *SCN1A* mutations databases (http://www.scn1a.info/; http://www.molgen.vib-ua.be/scn1amutations/). Further it was absent from the individuals of the 1000 genome and 5000 exome projects as well as from the 276,938 alleles of the gnomAD database.

The heterozygous p.N541S *SCN1A* variant had been inherited from her healthy mother (II:6) and was also present in one of the mother's unaffected brothers (II:3). This allows the assumption that the mutation was inherited from the patient's grandparents (I:1 or I:2) who were not available for genetic testing. Other potential disease mutations within a panel of genes presently known to cause epilepsy if mutated (n=350 on **Supplementary table 01**), especially those associated with West Syndrome could be excluded, either due to their frequency in healthy controls (of the 1000 Genome Project and the gnomAD Server) or due to an entirely distinct clinical phenotype (**Supplementary table 02**).

ANIMAL STUDIES

Heterozygous *Prg1*-mutant mice show neither juvenile seizures nor spiking pattern in the EEG.

In agreement with the previous reports on increased early postnatal neuronal network excitability (Vogt *et al*, 2017) and on juvenile hippocampal seizures (Trimbuch *et al*, 2009), *Prg1*$^{-/-}$ mutants (n=7) recorded on postnatal days 19-22 showed epileptiform activity in the cortical EEG and exhibited associated tonic-clonic or clonic motor seizures (4 of 7 mice, **Fig. 2**). One *Prg1*$^{-/-}$ mutant mouse died between P21-P22 in *status epilepticus*. Neither heterozygous *Prg1*$^{+/-}$ (n=7) nor wild type littermates (n=6) displayed pathological electrographic activity or spontaneous seizures (**Fig. 2**). Breeding observations of this mouse line for at least 24 months indicated that homozygous *Prg1*$^{-/-}$ animals, which survived the critical time period at around 3 weeks of age, remained henceforth clinically seizure-free until death.

Heterozygous *Prg1*-mutant mice show increased seizure susceptibility in adulthood.

Having shown that homozygous *Prg1*$^{-/-}$ mice had spontaneous seizures during early postnatal development, we investigated the potential of Prg1-haploinsufficiency to modify seizure susceptibility (**Fig. 3**). As heterozygous *Prg1*$^{+/-}$ mice did not seize spontaneously, we used an established kainate-model in adult animals (McLin & Steward, 2006). Since the *Prg1*-knockout animals are maintained on the congenic C57BL/6J background, which is especially resistant to kainate-induced seizures, we compared the susceptibility of the mutants to their

wildtype (wt) littermates. Only 7 out of 13 wt mice reached status epilepticus, which agrees with published data (McLin & Steward, 2006). After an initial kainate injection, heterozygous *Prg1*$^{+/-}$ and homozygous *Prg1*$^{-/-}$ mice exhibited significantly higher average seizure susceptibility scores than their wt littermates, in which epileptic activity was almost absent (**Fig. 3A**). In addition, *Prg1*$^{+/-}$ mice required significantly lower amounts of kainate to progress into their first epileptic seizure than their wildtype littermates (**Fig. 3B**). In fact, 23 out of 24 *Prg1*$^{+/-}$ mice and all (14 out of 14) *Prg1*$^{-/-}$ exhibited status epilepticus, which is in strong contrast to 7 out of 13 in the wildtype group (**Fig. 3C**). The body weight of the mice did not significantly differ between the groups (**Fig. 3D**). These data suggest that Prg1-haploinsufficiency significantly increases susceptibility for entry into status epilepticus, indicating that already a partial reduction of functional Prg1 at the synapse has important functional consequences for hippocampal network stability.

Double heterozygous *Prg1/Scn1a*-mutant mice show increased seizure susceptibility in adulthood.

We investigated the potential of *Prg1* haploinsufficiency to modify the epileptic phenotype of heterozygous *Scn1a*$^{wt/p.R1648H}$ mice by crossing both lines to obtain double heterozygous *Prg1*$^{+/-}$|*Scn1a*$^{wt/R1648H}$ mice (**Fig. 4**). Again, we used the established kainate-model in adult animals to induce seizures. Due to the importance of the genetic background affecting epileptic susceptibility (McLin & Steward, 2006), we analyzed wildtype littermates from the same breeding line as controls. All *Prg1*$^{+/-}$|*Scn1a*$^{wt/p.R1648H}$ mutants (13/13) developed epileptic seizures (stage 4) after an initial kainate dose, whereas only 3 out of 21 of the *Scn1a*$^{wt/p.R1648H}$ littermates did so. Also the epilepsy stage reached after an initial kainate dosage was significantly higher in double heterozygous *Prg1*$^{+/-}$|*Scn1a*$^{wt/p.R1648H}$ mice than in their *Scn1a*$^{wt/p.R1648H}$ or wildtype littermates suggesting higher seizure susceptibility in *Prg1*$^{+/-}$|*Scn1a*$^{wt/p.R1648H}$ mice. After an initial kainate injection, all but one heterozygous *Prg1*$^{+/-}$|*Scn1a*$^{wt/p.R1648H}$ mice directly proceeded to *status epilepticus* (SE), while *Scn1a*$^{wt/p.R1648H}$ or wildtype littermates required additional dosages to reach stage 5 criteria (SE), which is mirrored by the significant lower total amount of kainate necessary for *Prg1*$^{+/-}$|*Scn1a*$^{wt/p.R1648H}$ mice to progress into their first seizure (**Fig. 4B**). The higher seizure susceptibility of *Prg1*$^{+/-}$|*Scn1a*$^{wt/p.R1648H}$ mice is further reflected by the fact that 100% of these mice reached SE-criteria, while SE was reached by only 76% of the *Scn1a*$^{wt/p.R1648H}$ and 71% of their wildtype

littermates (**Fig. 4C**). No differences were observed in body weight between genotypes (**Fig. 4D**).

These data suggest that *Prg1*-haploinsufficiency significantly increases susceptibility for epileptic seizures in heterozygous *Scn1a*$^{wt/p.R1648H}$ mice.

ELECTROPHYSIOLOGY

The p.T300S mutation of Prg1 shows a loss-of-function effect in the mouse hippocampus.

To test the functional relevance of the human p.T299S missense mutation of *PRG1* on the cellular level, we performed electrophysiological experiments on acute hippocampal brain slices (**Fig. 5**) from *Prg1*$^{-/-}$ animals, into which we had either *in-utero* electroporated (**Fig. 5A,B**) a wildtype *Prg1-GFP* or a *Prg1*$^{p.T300S}$-GFP fusion construct (*nota bene*: the p.T300S mutation in mice corresponds to the p.T299S in humans). Such functional rescue on the cellular/neuronal level has been successfully demonstrated previously (Trimbuch *et al*, 2009). This approach allowed us to investigate the electrophysiological effects of re-expressed Prg1 in a small subset of GFP^{+} single neurons independent of the surrounding *Prg1*-knockout environment.

Whole cell patch-clamp recordings from GFP^{+}/Prg1^{+} and from GFP^{-}/Prg1$^{-/-}$ CA1 pyramidal neurons in acute hippocampal slices (**Fig. 5C**) showed a significant decrease of the *miniature Excitatory Postsynaptic Current* (mEPSC) frequency in the GFP^{+}/Prg1^{+} cells, indicating a functional rescue by electroporation of the Prg1-GFP fusion construct (GFP^{-}/Prg1$^{-/-}$, n=14; 3.32±0.43 Hz; GFP^{+}/Prg1^{+}, n=17; 1.86±0.13 Hz; unpaired two-tailed t-test: p=0.0014) (**Fig. 5D,E**).

Next we set out to test whether *in-utero* electroporation of GFP/Prg1-constructs with the mutation corresponding to human p.T299S were able to rescue the electrophysiological effects seen in the *Prg1*$^{-/-}$ neurons (**Fig. 5D,E**). Recordings of mEPSCs from GFP^{+}/Prg1$^{p.T300S}$ and GFP^{-}/Prg1$^{-/-}$ in CA1 pyramidal neurons did not show any significant differences in frequency (GFP^{-}/Prg1$^{-/-}$, n=9; 3.20±0.41 Hz; GFP^{+}/Prg1$^{p.T300S,}$ n=11; 2.98±0.26 Hz; p=0.32).

In the hippocampus, the neurons of the CA3 region are known to be crucially involved in epileptogenesis (Zhang *et al*, 2012). Hence we additionally performed whole cell patch-clamp recordings from hippocampal CA3 pyramidal neurons (**Fig. 5F,G**) and also found an mEPSC frequency that was significantly higher in *Prg1*$^{-/-}$ mice as compared to wildtype lit-

termates (2.47±0.32 Hz versus 5.15±0.64 Hz; unpaired two-tailed t-test: p=0.007). This confirms that loss of Prg1 function increased excitability in both CA1 and CA3 areas.

These results indicate that the construct corresponding to the human p.T299S mutation was unable to rescue Prg1 deficiency on the synaptic level. The persisting increase of excitatory glutamatergic transmission functionally confirms the loss-of-function of the human mutations.

DISCUSSION

In a previous study we show that homozygous Prg1-deficiency in mice resulted in neuronal hyperexcitability, early neuronal network synchronization, and seizures around postnatal days P18-21 (Vogt *et al*, 2017). Heterozygous *Prg1*$^{+/-}$ littermates had a normal EEG at resting state, but showed an increased susceptibility for epileptic seizures upon kainate stimulation. This indicates a sub-threshold increase of neuronal excitability caused by PRG1 haploinsufficiency.

To follow-up on these observations, we searched for *PRG1*-mutations in human patients with epilepsy. The decision, which cohorts to screen, was guided by the mouse phenotype: **(i)** Most homozygous *Prg1*$^{-/-}$ mice convulse around postnatal days P18-21. This corresponds to a human age of 6-9 months, if referring to fundamental dynamics of brain growth, circuit organization and myelination (Levitt, 2003). The *Prg1*$^{-/-}$ mice who survived their spontaneous *status epilepticus* lived on normally after P22 (verified by video monitoring), when seizures spontaneously ceased (Trimbuch *et al*, 2009). **(ii)** Prg1 is expressed in the mouse hippocampus during postnatal brain development (Bräuer *et al*, 2003; Unichenko *et al*, 2016), and **(iii)** the EEG of the *Prg1*$^{-/-}$ animals showed prominent irregular high-amplitude, slow-frequency discharges, multifocal spikes, and absent topical organization reminiscent of hypsarrhythmia, a hallmark of West syndrome (Dulac, 2001). We thus chose a cohort of 18 children with idiopathic West syndrome (infantile spasms).

In this cohort we found one child with a heterozygous *PRG1*-mutation resulting in the substitution of a serine for a threonine (p.T299S), which was absent in 400 Middle European control alleles, in 2,504 individuals of the 1000 genome project and present only once in heterozygous state in 122,802 individuals from the gnomAD server. Thr299 is located in the third extracellular domain in a motif that is highly evolutionary conserved in PRG1 and in other members of the LPP protein-family. Thr299 is located adjacent to Arg297, one of the critical amino acids for phospholipid interaction and de-phosphorylation of bioactive lipid-phosphates (Zhang *et al*, 2000). A similar mutation p.H253K, in the second extracellular domain that was previously introduced by *in utero* electroporation into embryonic mouse brains, disturbed the interaction between Prg1 with lysophosphatidic acid and to disrupt Prg1 function as shown by electrophysiological measurements (Trimbuch *et al*, 2009).

To establish whether the PRG1 p.T299S substitution affects protein function, we *in-utero* re-expressed the mouse homolog of the human mutation in neurons of *Prg1*$^{-/-}$ mutants and

investigated glutamatergic transmission in the hippocampus. Indeed, the altered p.T299S mutant Prg1 molecules were no longer able to control lipid signaling on the synaptic level in *Prg1*$^{-/-}$ neurons. This loss of function and subsequent dramatic increase in glutamatergic transmission would likely be a contributing factor to epileptogenesis, both in mice and in humans (Bianchi *et al*, 2012).

Guided by our mouse data, where Prg1-haploinsufficiency significantly increases susceptibility for epileptic seizures, we assumed a modifying effect of the *PRG1*-variant since this variant was inherited from an unaffected parent. Our hypothesis was strengthened by the discovery of an additional p.N541S *SCN1A* variant in our patient. In our family the impact of the *SCN1A* variant alone seems to be insufficient to cause epileptic seizures as this variant had been inherited from the clinically unaffected mother and was also found in another healthy family member (**Fig. 1A**). This mutation, which is not present in the *SCN1A* mutation databases or in the Human Genome Mutation Database (HGMD), was predicted to be disease-causing by the MutationTaster2 software with a probability of P=0.999. It was found only once in the heterozygous state amongst 245,604 alleles from the gnomAD database, a large gene mutation databases of non-epileptic individuals. With respect to pathogenicity of a *SCN1A* variant we are aware that a number of *SCN1A* variants in the HGMD database would not be classifiable as “clearly pathogenic”, and that, as recently pointed out, a significant fraction of patients identified with *SCN1A* mutations may actually not carry any *SCN1A* variant relevant for epileptogenesis (Lal *et al*, 2016). We agree with these authors that the role of *SCN1A* missense variants in the pathogenesis of common epilepsies should not be overstated. However, we want to point out that the pathogenicity of a certain variant does not only depend on the functional alteration of the protein in isolation, but also on the functional network in which the protein operates. In some cases this network might compensate for a minor dysfunction (as in the mother and the uncle of our patient) and in other cases not (as in our patient with West syndrome).

A number of studies provide compelling evidence for the presence of genetic modifiers. Miller *et al.* demonstrated that disease severity in *Scn1a* mutant mice strongly depends on the genetic background of the respective mouse strain and identified several modifier loci (Miller *et al*, 2014). Ohmori *et al.* reported that patients *with SCN1A* mutations plus certain *CACNA1A* variants had absence seizures more frequently than patients with *SCN1A* mutations alone and exhibited earlier seizure onset and prolonged seizure duration (Ohmori *et al*,

2013). Singh *et al.* proposed *SCN9A* as a genetic modifier of Dravet syndrome, whereby *SCN9A* may exacerbate the impact of *SCN1A* mutations on neuronal excitability (Singh *et al*, 2009). Despite these association studies, functional poof of a modifier for epilepsy in humans has not yet been provided. To study the effect of *Prg1*-mutations on a preexisting epileptic phenotype, we performed double mutant studies of *Prg1*$^{+/-}$ mice carrying an epilepsy-causing mutation in the $Na_v1.1$ sodium channel (*Scn1a*). This mutation has been previously identified in a large family exhibiting either febrile or afebrile generalized tonic–clonic or absence seizures (Escayg *et al*, 2000). The *SCNA1* mouse model recapitulates the human GEFS+ phenotype, showing spontaneous generalized seizures and a reduced threshold to thermally induced seizures even in a heterozygous state (Martin *et al*, 2010). Our epilepsy studies suggest a synergistic effect with respect to seizure susceptibility in Prg1-haploinsufficient mice additionally carrying an epilepsy-causing *Scn1a* mutation, a situation which in fact resembles the genetic background of our patient harboring two mutations in a heterozygous state.

Based on the functional data, we assume that a combined haploinsuffiency of *PRG1* and *SCN1A* might be potent enough to evoke a transient severe seizure phenotype in our patient. The p.N541S variant is located in the large cytoplasmic loop between the first and second transmembrane segments of the SCN1A channel, a region known to be sometimes tolerant to substitutions, even if the substitution affects an evolutionarily conserved residue (Lal *et al*, 2016). Hence this variant might only have a modest effect on channel function, illustrated by the fact the single *SCN1A* heterozygous individuals (**Fig. 1A**, II:3 and II:6) are seizure free, and its epileptogenic effect only becomes manifest in combination with the heterozygous *PRG1* mutation.

In summary, our clinical and functional data indicate that PRG1-haploinsufficiency mediates an increase in excitability, sufficient to modify a pre-existing epileptic phenotype resulting in apparent aggravation and eventually seizures, but is not sufficient to cause seizures by itself. We thus assume that heterozygous *PRG1*-mutations can act as a modifier of a pre-existing epileptic phenotype. Future studies will show, whether direct modulation of PRG1 or an indirect intervention *via* the blocking of LPA2-receptors might be a valuable pharmacological tool to treat juvenile forms of epilepsy. Using pharmacological intervention into phospholipid signaling, we were able to rescue the altered cortical somatosensory filter function in an animal model with monoallelic PRG1 deficiency pointing towards a new therapeutic ap-

proach against epilepsy, e.g. *via* modulation of phospholipid signaling by pharmacological inhibition of the LPA-synthesizing molecule autotoxin (Vogt *et al*, 2016) by an orally bioavailable small molecule PF-8380 (Gierse *et al*, 2010).

PATIENTS AND METHODS

Patient cohort

All patient-related studies were approved by the IRB of the Charité (EA1/215/08). All patients or caretakers provided written informed consent according to the Declaration of Helsinki. Guided by the timing of seizures and the EEG pattern of hypsarrhythmia, we selected a cohort of 18 patients suffering from idiopathic West syndrome with good outcome, who did not require antiepileptic drugs (AEDs) later in life. Brain malformations and metabolic disorders had been ruled out by appropriate imaging and metabolic studies.

Mutation screening in patients and control DNA samples

Genomic DNA was isolated from peripheral blood cells or from saliva by standard protocols. All coding exons of *PRG1* and 50 bp flanking intronic regions (GenBank NM_014839.4) were PCR-amplified and subjected to automatic sequencing with the BigDye® Terminator protocol (Applied Biosystems). Sequences were analyzed with the MutationSurveyor v3.10 (SoftGenetics) and the MutationTaster software (Schwarz *et al*, 2014). PCR conditions and oligonucleotide primer sequences are available upon request. The presence of the c.896C>G *PRG1*-mutation was verified in the patient and her family by restriction fragment length polymorphism (RFLP) analysis (**Fig. 1C**): The oligonucleotide primer pair (FORW) 5'-TTG GCA GGC ACA GAA CAT AG-3' and (REV) 5'-CGG CCA GAG ATT TTC TCA TT-3' amplified a 442 bp fragment from genomic DNA, which would cleaved by *Dde*I into fragments of 190+180+72 bp in the presence of the wildtype and 262+180 bp of the mutant allele. Absence of the mutation in 200 healthy controls from the same ethnic background was verified by the same assay.

Whole Exome Sequencing

Exonic sequences were enriched from genomic DNA of the patient (**Fig. 1A**, III:2) and her parents **(Fig. 1A**, II:6 and II:7) using the SureSelect® V4 Human All Exon 51 Mb Kit (Agilent Technologies). Sequencing was done on a HiSeq®2500 machine (Illumina), which produced between 43-62 million 100 bp paired-end reads. The combined paired-end FASTQ files were aligned to the human GRCh37.p11 (hg19/Ensembl 72) genomic sequence using the BWA-MEM V.0.7.1 aligner (Li, 2013). The raw alignments were fine-adjusted and called for deviations from the human reference sequence (GRCh37.p11) in all exonic ±50 bp flanking regions using the Genome Analysis Toolkit (GATK v3.8) software package (DePristo *et al*, 2011; McKenna *et al*, 2010). The resulting variant (VCF) files comprised ≈60-80.000 variants and

were sent to the MutationTaster2 Query Engine for assessment of the potential pathogenicity of all variants (Schwarz *et al*, 2014). Subsequent downstream analysis of potentially pathogenic variants was restricted to the 350 known epilepsy genes (**Supplementary table 01**). *De novo* mutations in the patient were screened for by trio-WES. Subsequently we compared the patient's variant calling (VCF) file to those of her parents using the '--mendel' option of the VCFtools v0.1.14 software package to search for variants that were present in the patient, but not in her parents (Danecek *et al*, 2011).

Animal studies

The animal studies were approved by the local animal welfare committee (LaGeSo T0100/03 & G0433/09, as well as G-12-096). We used male heterozygous *Prg1*$^{-/+}$, homozygous *Prg1*$^{-/-}$ (Trimbuch *et al*, 2009), heterozygous *Scn1a*$^{wt/p.R1648H}$ (Hedrich *et al*, 2014; Martin *et al*, 2010), and double heterozygous *Prg1*$^{-/+}$|*Scn1a*$^{wt/p.R1648H}$ mutant mice on a C57BL/6J genetic background along with their wildtype littermates. In humans, the heterozygous p.R1648H mutation in SCN1A causes a GEFS+ phenotype (Escayg *et al*, 2000). Mice were kept under SPF-conditions with a 12 h dark/light cycle, had *ad libitum* access to food and water and were kept and euthanized in accordance with national regulations.

EEG recordings in freely moving animals using implanted epidural electrodes

Single tungsten wires (40 µm, California Fine Wire) were implanted into P18 pups under isoflurane anesthesia. Craniotomies were performed without damaging the underlying dura. Electrodes were placed bilaterally at 2.0 mm posterior from bregma and 3.0 mm lateral from midline with a reference electrode above the cerebellum (Trimbuch *et al*, 2009). Implanted electrodes were secured on the skull with dental acrylic. During recordings electrodes were connected to operational preamplifiers to eliminate cable movement artifacts. Electrophysiological signals were differentially amplified, band-pass filtered (1 Hz-10 kHz) and acquired continuously at 32 kHz (Neuralynx). Recordings were performed on freely moving animals at P19-P22 in 19 x 29 cm Plexiglas cages. EEG was obtained by low-pass filtering and down-sampling of the wide-band signal to 1,250 Hz. Mice were monitored from different angles by two video cameras.

Seizure induction with kainic acid

Adult male 3-months-old wildtype (n=13), hetero- (n=24), and homozygous (n=14) *Prg1*-mutant (Trimbuch *et al*, 2009) littermates as well as *Scn1a*$^{wt/p.R1648H}$ heterozygous (n=21) (Hedrich *et al*, 2014; Martin *et al*, 2010), *Prg1*$^{+/-}$|*Scn1a*$^{wt/p.R1648H}$ double-heterozygous (n=13),

and wildtype littermates (n=14) were analyzed for susceptibility to cerebral seizures. The susceptibility for epileptic seizures was assessed following established protocols (McLin & Steward, 2006). Briefly, animals were initially injected with 20 mg/kg kainate (at a concentration of 5 mg/ml) and assessed for 45 minutes. After this period, animals were given additional doses of kainate (14 mg/kg) at a 45 min interval (or at a 60 minutes interval after reaching level 4 seizures) and were assessed every 5 minutes. According to standard criteria from previous reports (McLin & Steward, 2006), only mice who exhibited level 5 seizures (*status epilepticus* characterized by repetitive, tonic-clonic seizures for at least 2 observation intervals longer than 10 min) during the 4 h evaluation period were included into this study.- Epileptic susceptibility (reaching stage 5) was assessed on a binary (yes/no) basis. Seizure stage was evaluated according to an established six-point scale (McLin & Steward, 2006). Epilepsy stages were evaluated by at least two independent investigators who were blinded for the genotypes. After the experiments animals tail cuts were genotyped and corresponding genotypes were assigned.

***In-utero* electroporation**

The *in-utero* electroporation experiments in embryos from $Prg1^{+/-}$ x $Prg1^{+/-}$ matings were carried out in accordance with a protocol approved by the local animal welfare committee as described before (Prozorovski *et al*, 2008). The wt and mutant *Prg1-GFP* plasmids (Trimbuch *et al*, 2009) were prepared at a concentration of 4 µg/µl using the EndoFree Plasmid Kit (Qiagen). We used mice from timed matings at E15-E16 (*post coitum*). After anesthesia with 10 mg/ml ketamine and 1 mg/ml xylazine, the uterine horns were exposed. The DNA solution (1.0-1.5 µl/embryo) was injected through the uterine wall into the lateral ventricle of two of the embryos by pulled glass capillaries (WPI). Electric pulses were delivered to embryos by holding the injected brain through the uterine wall with forceps-type electrodes (CUY650P5) connected to a square-pulse generator (CUY 21 Edit, Unique Medical Imada). Five 38 V pulses of 50 ms were applied at 950 ms intervals. The uterine horns were carefully replaced into the abdominal cavity before the muscle wall and skin were sutured. Animals were checked for the $Prg1^{-/-}$ phenotype after birth and the efficacy of *in-utero* electroporation was assessed by visualization of the GFP-fluorescence signal, whose coding sequence was also present on the electroporated plasmid.

Electrophysiology

P20-mice were anesthetized with isoflurane and decapitated. Brains were quickly removed and chilled in ice-cold, oxygenated, sucrose based artificial cerebrospinal fluid (sACSF) containing [in mM]: NaCl [87], $NaHCO_3$ [26], sucrose [75], glucose [25], KCl [2·4], NaH_2PO_4 [1.25], $MgCl_2$ [7], and $CaCl_2$ [0.5] at 350±10 mOsm. Horizontal 300 µm slices were cut using a Leica VT1200 Vibratome (Leica Microsystems). Slices were then incubated for 30 min at 35°C in sACSF and afterwards stored at room temperature in normal ACSF containing [in mM]: NaCl [119], $NaHCO_3$ [26], glucose [10], KCl [2.5], NaH_2PO_4 [1.25], $MgCl_2$ [1.3] and $CaCl_2$ [2.5]; pH 7.4 at 300±10 mOsm. Normal ACSF was also used for recordings. All solutions were constantly equilibrated with carbogen (95% O_2|5% CO_2).

Whole-cell voltage-clamp recordings were performed with an Axopatch 700B amplifier (Axon Instruments) and filtered at 2 kHz. Data were digitized (BNC-2090, National Instruments) at 5-10 kHz, recorded and analyzed with custom-made software in IGOR Pro (WaveMetrics). For whole-cell recordings, borosilicate glass electrodes (2-5 MΩ) were filled with [in mM]: K-gluconate [135], HEPES [10], Mg-ATP [2], KCl [20], EGTA [0·2], and spH was adjusted to 7.2 with KOH. Series resistance (Rs) was monitored throughout experiments; cells were rejected if Rs was >30 MΩ or varied >±30% during the recording. No Rs compensation was used. Whole-cell recordings were performed in the presence of the $GABA_A$ receptor-antagonists Gabazine [1 µM] (SR 95531, Sigma-Aldrich). For the recording of miniature excitatory postsynaptic currents (mEPSCs) 2 µM Tetrodotoxin (TTX), 50 µM D-(-)-2-Amino-5-phosphonopentanoic acid (D-AP5) and 100 µM Cyclothiazide (all drugs purchased from Tocris Bioscience) were added to the recording solution.

Data analysis

Data was assessed for normal distribution and was analyzed accordingly. For group comparisons a nonparametric Kruskal-Wallis test was used. Non-parametric data were analyzed using the Mann-Whitney U-test. Post-hoc analysis was performed using the Dunn's multiple comparison test. Pearson's χ^2 was used for dichotomous (present/absent) values. Miniature EPSCs were detected using a threshold algorithm generated in MatLab and/or Igor plug-in NeuroMatics and statistical significance was assessed with a Student's t-test.

ACKNOWLEDGMENTS

We thank the patient's family for participation in this study. This work was supported by grants of the Deutsche Forschungsgemeinschaft (SFB 665 to Markus Schuelke, Robert Nitsch, Dietmar Schmitz; SFB 1080 to Robert Nitsch and Johannes Vogt, and SFB 1193 to Johannes Vogt), the European Research Council (ERC-AG "LiPsyD" to Robert Nitsch), the Stiftung Charité, and the NeuroCure Cluster of Excellence of the DFG (Exc 257) to Tatiana Korotkova, Alexey Ponomarenko, Dietmar Schmitz, Markus Schuelke.

AUTHOR CONTRIBUTIONS

Investigated the patients, analyzed the human molecular genetics data (EK, MS); contributed to the patient cohort and patient phenotypes (AP, US); performed neurophysiologic studies (MK, AP, JB, PB, TK, TT); performed molecular genetics experiments (EK, MS, TT); performed the kainate experiments (JV, RN); contributed materials and animals (AE, HL); performed *in utero* electroporation (JV, JB); wrote the first draft of the manuscript (EK, JV, MS); jointly supervised the research (RN, DS, MS); read the final version of the manuscript and consented to its publication (all authors).

CONFLICT OF INTEREST

The authors do not report any conflicts of interest.

REFERENCES

Appenzeller S, Balling R, Barisic N, Baulac S, Caglayan H, Craiu D, De Jonghe P, Depienne C, Dimova P, Djémié T, Gormley P, Guerrini R, Helbig I, Hjalgrim H, Hoffman-Zacharska D, Jähn J, Klein KM, Koeleman B, Komarek V, Krause R, et al (2014) De Novo Mutations in Synaptic Transmission Genes Including DNM1 Cause Epileptic Encephalopathies. *Am. J. Hum. Genet.* **95:** 360–370

Banerjee PN, Filippi D & Allen Hauser W (2009) The descriptive epidemiology of epilepsy—A review. *Epilepsy Res.* **85:** 31–45

Baulac S, Huberfeld G, Gourfinkel-An I, Mitropoulou G, Beranger A, Prud'homme JF, Baulac M, Brice A, Bruzzone R & LeGuern E (2001) First genetic evidence of GABA(A) receptor dysfunction in epilepsy: a mutation in the gamma2-subunit gene. *Nat. Genet.* **28:** 46–48

Bianchi R, Wong RKS & Merlin LR (2012) Glutamate Receptors in Epilepsy: Group I mGluR-Mediated Epileptogenesis. In *Jasper's Basic Mechanisms of the Epilepsies*, Noebels JL Avoli M Rogawski MA Olsen RW & Delgado-Escueta AV (eds) Bethesda (MD): National Center for Biotechnology Information (US) Available at: http://www.ncbi.nlm.nih.gov/books/NBK98136/ [Accessed January 23, 2015]

Bräuer AU, Savaskan NE, Kühn H, Prehn S, Ninnemann O & Nitsch R (2003) A new phospholipid phosphatase, PRG-1, is involved in axon growth and regenerative sprouting. *Nat. Neurosci.* **6:** 572–578

Calhoun JD, Hawkins NA, Zachwieja NJ & Kearney JA (2017) Cacna1g is a genetic modifier of epilepsy in a mouse model of Dravet syndrome. *Epilepsia* **58:** e111–e115

Danecek P, Auton A, Abecasis G, Albers CA, Banks E, DePristo MA, Handsaker RE, Lunter G, Marth GT, Sherry ST, McVean G & Durbin R (2011) The variant call format and VCFtools. *Bioinformatics* **27:** 2156–2158

Depienne C, Trouillard O, Gourfinkel-An I, Saint-Martin C, Bouteiller D, Graber D, Barthez-Carpentier M-A, Gautier A, Villeneuve N, Dravet C, Livet M-O, Rivier-Ringenbach C, Adam C, Dupont S, Baulac S, Héron D, Nabbout R & LeGuern E (2010) Mechanisms for variable expressivity of inherited SCN1A mutations causing Dravet syndrome. *J. Med. Genet.* **47:** 404–410

DePristo MA, Banks E, Poplin R, Garimella KV, Maguire JR, Hartl C, Philippakis AA, del Angel G, Rivas MA, Hanna M, McKenna A, Fennell TJ, Kernytsky AM, Sivachenko AY, Cibulskis K, Gabriel SB, Altshuler D & Daly MJ (2011) A framework for variation discovery and genotyping using next-generation DNA sequencing data. *Nat. Genet.* **43:** 491–498

Dichgans M, Freilinger T, Eckstein G, Babini E, Lorenz-Depiereux B, Biskup S, Ferrari MD, Herzog J, van den Maagdenberg AM, Pusch M & Strom TM (2005) Mutation in the neuronal voltage-gated sodium channel SCN1A in familial hemiplegic migraine. *The Lancet* **366:** 371–377

Dulac O (2001) What is West syndrome? *Brain Dev.* **23:** 447–452

Escayg A & Goldin AL (2010) Sodium channel SCN1A and epilepsy: Mutations and mechanisms. *Epilepsia* **51:** 1650–1658

Escayg A, MacDonald BT, Meisler MH, Baulac S, Huberfeld G, An-Gourfinkel I, Brice A, LeGuern E, Moulard B, Chaigne D, Buresi C & Malafosse A (2000) Mutations of SCN1A, encoding a neuronal sodium channel, in two families with GEFS+2. *Nat. Genet.* **24:** 343–345

Frankel WN, Mahaffey CL, McGarr TC, Beyer BJ & Letts VA (2014) Unraveling Genetic Modifiers in the Gria4 Mouse Model of Absence Epilepsy. *PLOS Genet.* **10:** e1004454

Gheyara AL, Ponnusamy R, Djukic B, Craft RJ, Ho K, Guo W, Finucane MM, Sanchez PE & Mucke L (2014) Tau reduction prevents disease in a mouse model of Dravet syndrome. *Ann. Neurol.* **76:** 443–456

Gierse J, Thorarensen A, Beltey K, Bradshaw-Pierce E, Cortes-Burgos L, Hall T, Johnston A, Murphy M, Nemirovskiy O, Ogawa S, Pegg L, Pelc M, Prinsen M, Schnute M, Wendling J, Wene S, Weinberg R, Wittwer A, Zweifel B & Masferrer J (2010) A Novel Autotaxin Inhibitor Reduces Lysophosphatidic Acid Levels in Plasma and the Site of Inflammation. *J. Pharmacol. Exp. Ther.* **334:** 310–317

Hedrich UBS, Liautard C, Kirschenbaum D, Pofahl M, Lavigne J, Liu Y, Theiss S, Slotta J, Escayg A, Dihné M, Beck H, Mantegazza M & Lerche H (2014) Impaired Action Potential Initiation in GABAergic Interneurons Causes Hyperexcitable Networks in an Epileptic Mouse Model Carrying a Human NaV1.1 Mutation. *J. Neurosci.* **34:** 14874–14889

Holth JK, Bomben VC, Reed JG, Inoue T, Younkin L, Younkin SG, Pautler RG, Botas J & Noebels JL (2013) Tau Loss Attenuates Neuronal Network Hyperexcitability in Mouse and Drosophila Genetic Models of Epilepsy. *J. Neurosci.* **33:** 1651–1659

Kearney JA, Yang Y, Beyer B, Bergren SK, Claes L, DeJonghe P & Frankel WN (2006) Severe epilepsy resulting from genetic interaction between Scn2a and Kcnq2. *Hum. Mol. Genet.* **15:** 1043–1048

Lal D, Reinthaler EM, Dejanovic B, May P, Thiele H, Lehesjoki A-E, Schwarz G, Riesch E, Ikram MA, van Duijn CM, Uitterlinden AG, Hofman A, Steinböck H, Gruber-Sedlmayr U, Neophytou B, Zara F, Hahn A, Genetic Commission of the Italian League against Epilepsy, EuroEPINOMICS CoGIE Consortium, Gormley P, et al (2016) Evaluation of Presumably Disease Causing SCN1A Variants in a Cohort of Common Epilepsy Syndromes. *PloS One* **11:** e0150426

Lek M, Karczewski KJ, Minikel EV, Samocha KE, Banks E, Fennell T, O'Donnell-Luria AH, Ware JS, Hill AJ, Cummings BB, Tukiainen T, Birnbaum DP, Kosmicki JA, Duncan LE, Estrada K, Zhao F, Zou J, Pierce-Hoffman E, Berghout J, Cooper DN, et al (2016) Analysis of protein-coding genetic variation in 60,706 humans. *Nature* **536:** 285–291

Levitt P (2003) Structural and functional maturation of the developing primate brain. *J. Pediatr.* **143:** S35-45

Li H (2013) Aligning sequence reads, clone sequences and assembly contigs with BWA-MEM. **http://arxiv.org/pdf/1303.3997.pdf:** (accessed at Sept 2015)

Liu X, Huai J, Endle H, Schlüter L, Fan W, Li Y, Richers S, Yurugi H, Rajalingam K, Ji H, Cheng H, Rister B, Horta G, Baumgart J, Berger H, Laube G, Schmitt U, Schmeisser MJ, Boeckers TM, Tenzer S, et al (2016) PRG-1 Regulates Synaptic Plasticity via Intracellular PP2A/β1-Integrin Signaling. *Dev. Cell* **38:** 275–290

Martin MS, Dutt K, Papale LA, Dubé CM, Dutton SB, Haan G de, Shankar A, Tufik S, Meisler MH, Baram TZ, Goldin AL & Escayg A (2010) Altered Function of the SCN1A Voltage-gated Sodium Channel Leads to γ-Aminobutyric Acid-ergic (GABAergic) Interneuron Abnormalities. *J. Biol. Chem.* **285:** 9823–9834

McKenna A, Hanna M, Banks E, Sivachenko A, Cibulskis K, Kernytsky A, Garimella K, Altshuler D, Gabriel S, Daly M & DePristo MA (2010) The Genome Analysis Toolkit: A MapReduce framework for analyzing next-generation DNA sequencing data. *Genome Res.* **20:** 1297–1303

McLin JP & Steward O (2006) Comparison of seizure phenotype and neurodegeneration induced by systemic kainic acid in inbred, outbred, and hybrid mouse strains. *Eur. J. Neurosci.* **24:** 2191–2202

Miller AR, Hawkins NA, McCollom CE & Kearney JA (2014) Mapping genetic modifiers of survival in a mouse model of Dravet syndrome. *Genes Brain Behav.* **13:** 163–172

Noebels J (2015) Pathway-driven discovery of epilepsy genes. *Nat. Neurosci.* **18:** 344

Noebels J (2017) Precision physiology and rescue of brain ion channel disorders. *J. Gen. Physiol.* **149:** 533–546

Ohmori I, Ouchida M, Kobayashi K, Jitsumori Y, Mori A, Michiue H, Nishiki T, Ohtsuka Y & Matsui H (2013) CACNA1A variants may modify the epileptic phenotype of Dravet syndrome. *Neurobiol. Dis.* **50:** 209–217

Oyrer J, Maljevic S, Scheffer IE, Berkovic SF, Petrou S & Reid CA (2018) Ion Channels in Genetic Epilepsy: From Genes and Mechanisms to Disease-Targeted Therapies. *Pharmacol. Rev.* **70:** 142–173

Prozorovski T, Schulze-Topphoff U, Glumm R, Baumgart J, Schröter F, Ninnemann O, Siegert E, Bendix I, Brüstle O, Nitsch R, Zipp F & Aktas O (2008) Sirt1 contributes critically to the redox-dependent fate of neural progenitors. *Nat. Cell Biol.* **10:** 385–394

Schwarz JM, Cooper DN, Schuelke M & Seelow D (2014) MutationTaster2: mutation prediction for the deep-sequencing age. *Nat. Methods* **11:** 361–362

Singh NA, Charlier C, Stauffer D, DuPont BR, Leach RJ, Melis R, Ronen GM, Bjerre I, Quattlebaum T, Murphy JV, McHarg ML, Gagnon D, Rosales TO, Peiffer A, Anderson VE & Leppert M (1998) A novel potassium channel gene, KCNQ2, is mutated in an inherited epilepsy of newborns. *Nat. Genet.* **18:** 25–29

Singh NA, Pappas C, Dahle EJ, Claes LRF, Pruess TH, De Jonghe P, Thompson J, Dixon M, Gurnett C, Peiffer A, White HS, Filloux F & Leppert MF (2009) A Role of SCN9A in Human Epilepsies, As a Cause of Febrile Seizures and As a Potential Modifier of Dravet Syndrome. *PLoS Genet* **5:** e1000649

Steinlein OK, Mulley JC, Propping P, Wallace RH, Phillips HA, Sutherland GR, Scheffer IE & Berkovic SF (1995) A missense mutation in the neuronal nicotinic acetylcholine receptor alpha 4 subunit is associated with autosomal dominant nocturnal frontal lobe epilepsy. *Nat. Genet.* **11:** 201–203

Trimbuch T, Beed P, Vogt J, Schuchmann S, Maier N, Kintscher M, Breustedt J, Schuelke M, Streu N, Kieselmann O, Brunk I, Laube G, Strauss U, Battefeld A, Wende H, Birchmeier C, Wiese S, Sendtner M, Kawabe H, Kishimoto-Suga M, et al (2009) Synaptic PRG-1 Modulates Excitatory Transmission via Lipid Phosphate-Mediated Signaling. *Cell* **138:** 1222–1235

Unichenko P, Kirischuk S, Yang J-W, Baumgart J, Roskoden T, Schneider P, Sommer A, Horta G, Radyushkin K, Nitsch R, Vogt J & Luhmann HJ (2016) Plasticity-Related Gene 1 Affects Mouse Barrel Cortex Function via Strengthening of Glutamatergic Thalamocortical Transmission. *Cereb. Cortex* **26:** 3260–3272

Vogt J, Kirischuk S, Unichenko P, Schlüter L, Pelosi A, Endle H, Yang J-W, Schmarowski N, Cheng J, Thalman C, Strauss U, Prokudin A, Bharati BS, Aoki J, Chun J, Lutz B, Luhmann HJ & Nitsch R (2017) Synaptic Phospholipid Signaling Modulates Axon Outgrowth via Glutamate-dependent Ca2+-mediated Molecular Pathways. *Cereb. Cortex* **27:** 131–145

Vogt J, Yang J-W, Mobascher A, Cheng J, Li Y, Liu X, Baumgart J, Thalman C, Kirischuk S, Unichenko P, Horta G, Radyushkin K, Stroh A, Richers S, Sahragard N, Distler U, Tenzer S, Qiao L, Lieb K, Tüscher O, et al (2016) Molecular cause and functional impact of altered synaptic lipid signaling due to a prg-1 gene SNP. *EMBO Mol. Med.* **8:** 25–38

Wallace RH, Marini C, Petrou S, Harkin LA, Bowser DN, Panchal RG, Williams DA, Sutherland GR, Mulley JC, Scheffer IE & Berkovic SF (2001) Mutant GABA(A) receptor gamma2-subunit in childhood absence epilepsy and febrile seizures. *Nat. Genet.* **28:** 49–52

Yu FH, Mantegazza M, Westenbroek RE, Robbins CA, Kalume F, Burton KA, Spain WJ, McKnight GS, Scheuer T & Catterall WA (2006) Reduced sodium current in GABAergic interneurons in a mouse model of severe myoclonic epilepsy in infancy. *Nat. Neurosci.* **9:** 1142–1149

Zhang Q, Pilquil C, Dewald, Berthiaume L & Brindley D (2000) Identification of structurally important domains of lipid phosphate phosphatase-1: implications for its sites of action. Available at: http://www.biochemj.org/bj/345/0181/bj3450181.htm [Accessed January 23, 2015]

Zhang W, Huguenard JR & Buckmaster PS (2012) Increased Excitatory Synaptic Input to Granule Cells from Hilar and CA3 Regions in a Rat Model of Temporal Lobe Epilepsy. *J. Neurosci.* **32:** 1183–1196

FIGURE LEGENDS

Figure 1: Pedigree of the family and molecular findings.

A Pedigree of the three generation family in whom one child (III:2) was affected with West syndrome. The genotypes with respect to the *SCNA1* and *PRG1*-mutations are provided below the symbols.

B Sequence electropherograms for *SCNA1* and *PRG1*-mutations in the index patient (lower panel) and a control (upper panel).

C Verification of the *PRG1*-mutation by RFLP analysis where the c.896C>G mutation abolishes a *Dde*I endonuclease restriction site.

D The multiple species amino acid sequence alignments of PRG1 and of SCN1A demonstrate the evolutionary conservation of both residues and their neighboring amino acids. The mutated amino acids are highlighted.

E Putative structure with 6 transmembrane domains and 3 extracellular loops. The specific domains for the interaction of lipid phosphate phosphatases with lipid phosphates are highlighted in red (D1-D3). The p.T299S mutation is located in the specific D3 domain of PRG1.

Figure 2: EEG recording and lack of spontaneous seizures in $Prg1^{+/-}$ mice.

A Examples of cortical EEG recorded in freely moving $Prg1^{-/-}$, $Prg1^{+/-}$, and wildtype $Prg1^{+/+}$ littermates on postnatal days P19-21. $Prg1^{+/-}$ and $Prg1^{+/+}$ mice showed normal EEG, while $Prg1^{-/-}$ mice displayed progressive aggravation of seizures up to lethal status epilepticus on day P21.

B A hypersynchronous EEG pattern recorded on P21 in another $Prg1^{-/-}$ mouse (left), power spectrum of this epoch (right) and a magnified slow potential with the concurrent gamma-band (~50 Hz) oscillation (gray inset). These patterns were not observed in either $Prg1^{+/+}$ or $Prg1^{+/-}$ mice.

C A snapshot from the video monitoring of motor activity performed simultaneously with EEG acquisition in a $Prg1^{+/-}$ mouse.

Figure 3: Epileptic susceptibility of adult *$Prg1^{+/-}$* and *$Prg1^{-/-}$* mice after kainate injection. *Nota bene*: as the genetic background of the mice plays an important role with regard to the

seizure susceptibility upon kainate injection (McLin & Steward, 2006), the control animals in this experiment were hence always taken from wildtype littermates.

A The epilepsy stage reached after an initial kainate dosage was significantly higher in heterozygous $Prg1^{+/-}$ (n=24) and homozygous $Prg1^{-/-}$ mice (n=14) than in their wildtype littermates (n=13).

B In line with higher susceptibility to the initial dose, heterozygous $Prg1^{+/-}$ (n=23) and homozygous $Prg1^{-/-}$ mice (n=14) needed lower amounts of kainate to evoke epileptic seizures (stage 4).

C Epileptic susceptibility assessed by the ability of the mice to reach a status epilepticus (SE=stage 5): only 53% of wildtype mice reached stage 5 while most (>95%) of the heterozygous and all (100%) of the homozygous *Prg1*-mutant mice reached *status epilepticus*.

D To avoid bias by confounders, we compared the body weights between the tested groups but did not find any significant differences. Statistical analyses for panels A, B, and D were performed using the nonparametric Kruskal-Wallis with post hoc Dunn's test, for panel C with the Pearson's χ^2 test. Error bars depict the SEM; significance levels: *, p<0.05; ** <.0.01; ****, p<0.001; *****, p<0.0001.

Figure 4: Epileptic susceptibility of adult *Scn1a*$^{wt/p.R1648H}$, and *Prg1*$^{+/-}$|*Scn1a*$^{wt/p.R1648H}$ double heterozygous mice after kainate injection. *Nota bene*: as the genetic background of the mice plays an important role with regard to the seizure susceptibility upon kainate injection (McLin & Steward, 2006), the control animals in this experiment were always taken from wildtype littermates.

A The epilepsy stage reached after an initial kainate dosage was significantly higher in double heterozygous *Prg1*$^{+/-}$|*Scn1a*$^{wt/p.R1648H}$ mice (n=13) in comparison to heterozygous *Scn1a*$^{wt/p.R1648H}$ mice (n=16) alone.

B There was no significant difference between heterozygous *Scn1a*$^{wt/p.R1648H}$ (n=16) and heterozygous *Prg1*$^{+/-}$|*Scn1a*$^{wt/p.R1648H}$ (n=13) mice with regard to reach epileptic seizures in response to the initial kainate dose.

C Epileptic susceptibility assessed by the ability of the mice to reach a *status epilepticus* (SE = stage 5): only 76% of wildtype littermates reached SE while 76% of the *Scn1a*$^{wt/p.R1648H}$ and 100% of *Prg1*$^{+/-}$|*Scn1a*$^{wt/p.R1648H}$ mice did so.

D To avoid bias by confounders, we compared the body weights between the tested groups but did not find any significant differences. Statistical analyses for panels A, B, and D were performed using the nonparametric Kruskal-Wallis with post hoc Dunn's test, for panel C with the Pearson's χ^2 test. Error bars depict the SEM; significance levels: *, p<0.05; ** <.0.01; ****, p<0.001; *****, p<0.0001.

Figure 5: Functional testing of the Prg1 p.T300S mutation using *in-utero* electroporation and electrophysiology.

A Scheme for *in-utero* electroporation (IUE), in which the gene of interest was introduced at E15.

B Hippocampal slice from an IUE mouse showing the different regions. A subset of CA1 cells were successfully electroporated with the gene of interest that was GFP-tagged for visualization.

C Recording configuration used for the miniature currents. Neighboring CA1 pyramidal cells of which one was electroporated (green, Ep) and the other non-electroporated (NonEp) were recorded.

D Representative traces showing mEPSCs in $Prg1^{-/-}$ (white circle), Prg1 rescued (grey circle), and $Prg1^{p.T300S}$ (green circle) electroporated neurons.

E Reexpression of Prg1 in $Prg1^{-/-}$ neurons significantly decreased mEPSC when compared to neighboring $Prg1^{-/-}$ neurons, which corresponds to a functional rescue as shown previously (Trimbuch *et al*, 2009). However, no differences in mEPSCs frequencies were observed between neighboring knockout $Prg1^{-/-}$ neurons and $Prg1^{p.T300S}$ electroporated CA1 pyramidal cells. mEPSC frequencies are plotted for $Prg1^{-/-}$ neurons and *in-utero* electroporated $Prg1^{-/-}$ neurons expressing Prg1, and $Prg1^{p.T300S}$ respectively. The n-numbers of investigated neurons of the respective genotypes are printed on the bars. Error bars depict the SEM.

F-G Also in hippocampal area CA3 the mEPSC frequency was significantly higher in $Prg1^{-/-}$ mice as compared to wildtype mice. Representative traces of wildtype (black circle) and $Prg1^{-/-}$ mice (white circle).

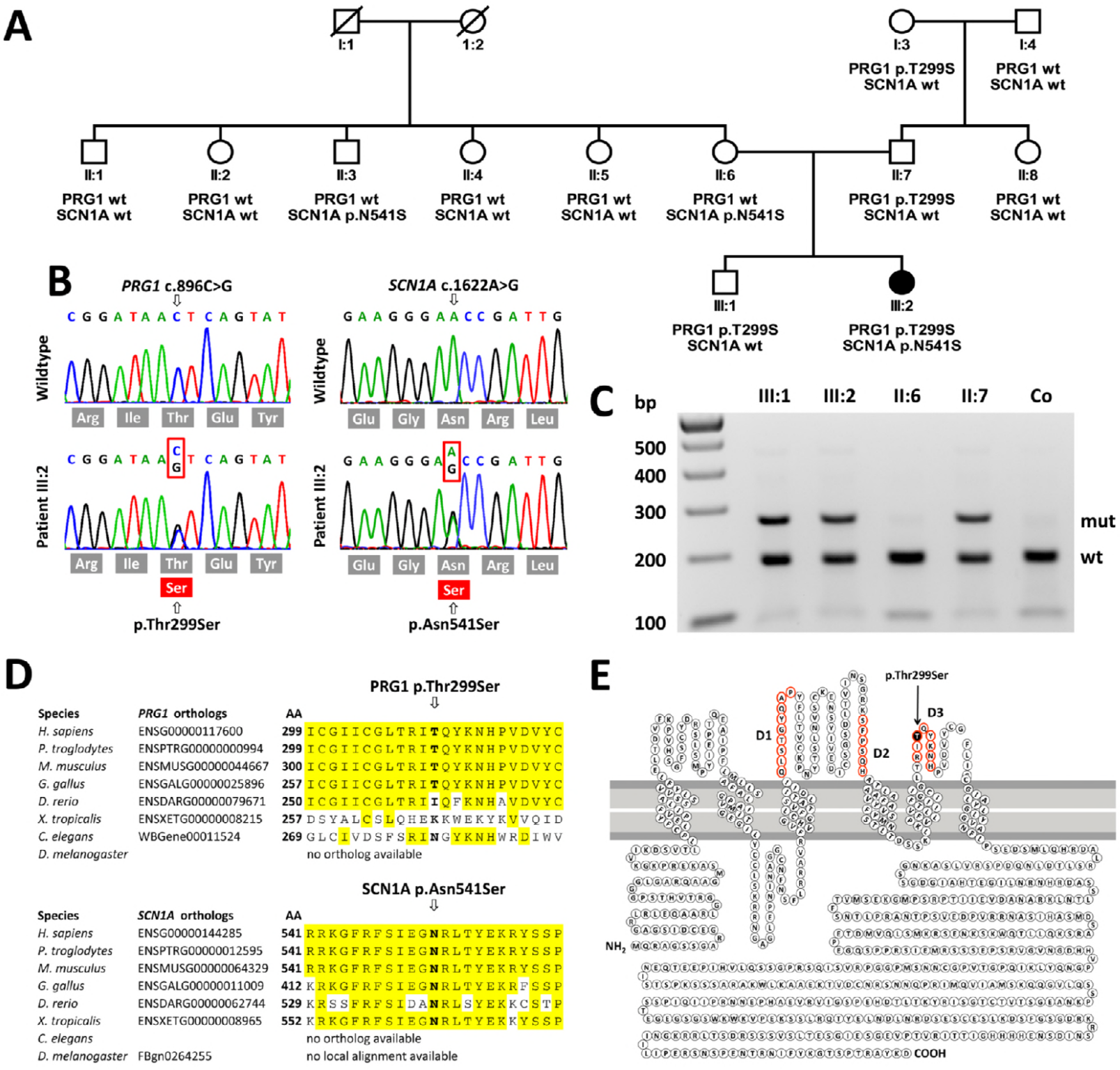

Knierim *et al.*, Figure 1

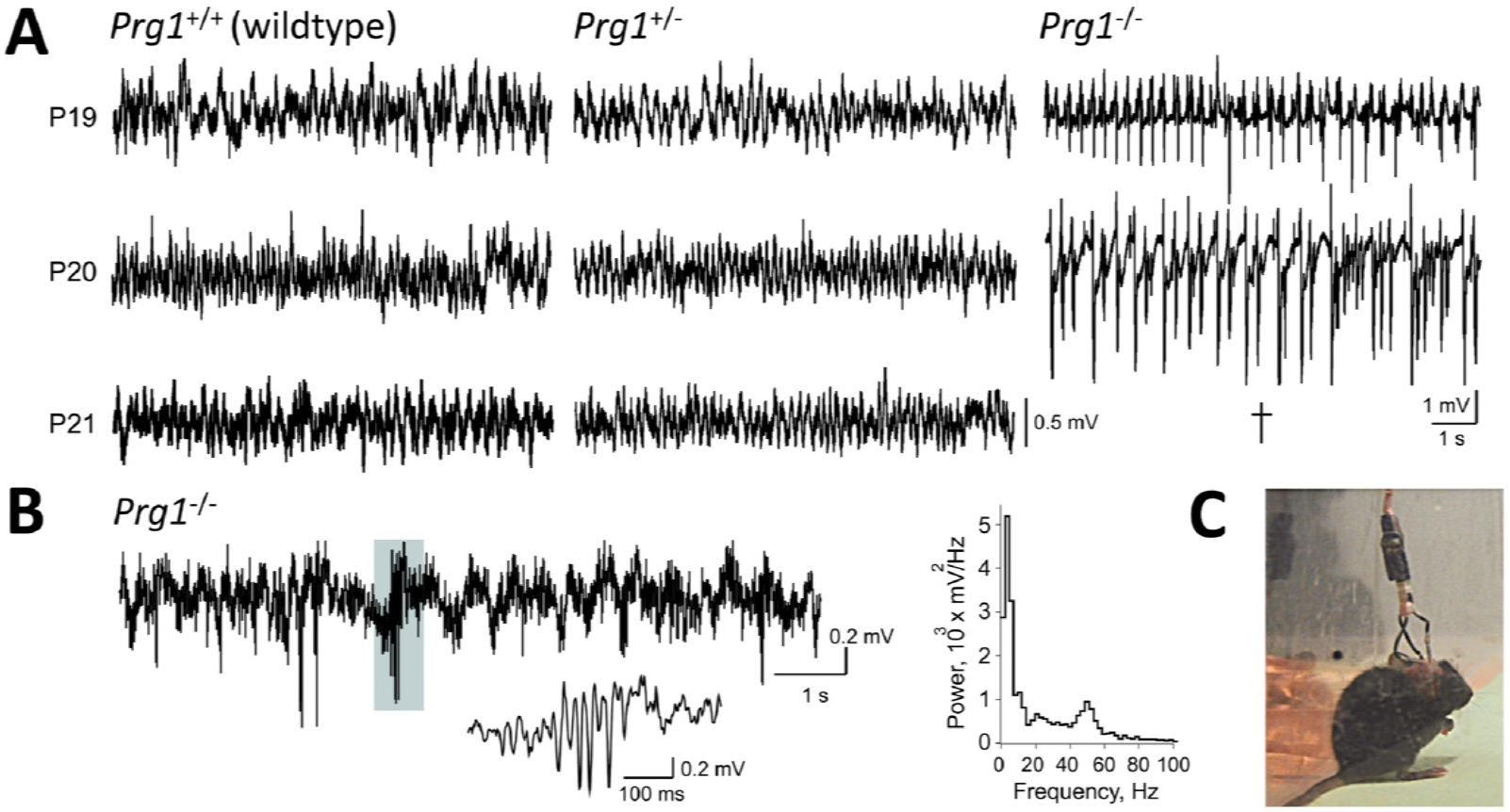

Knierim *et al.*, Figure 2

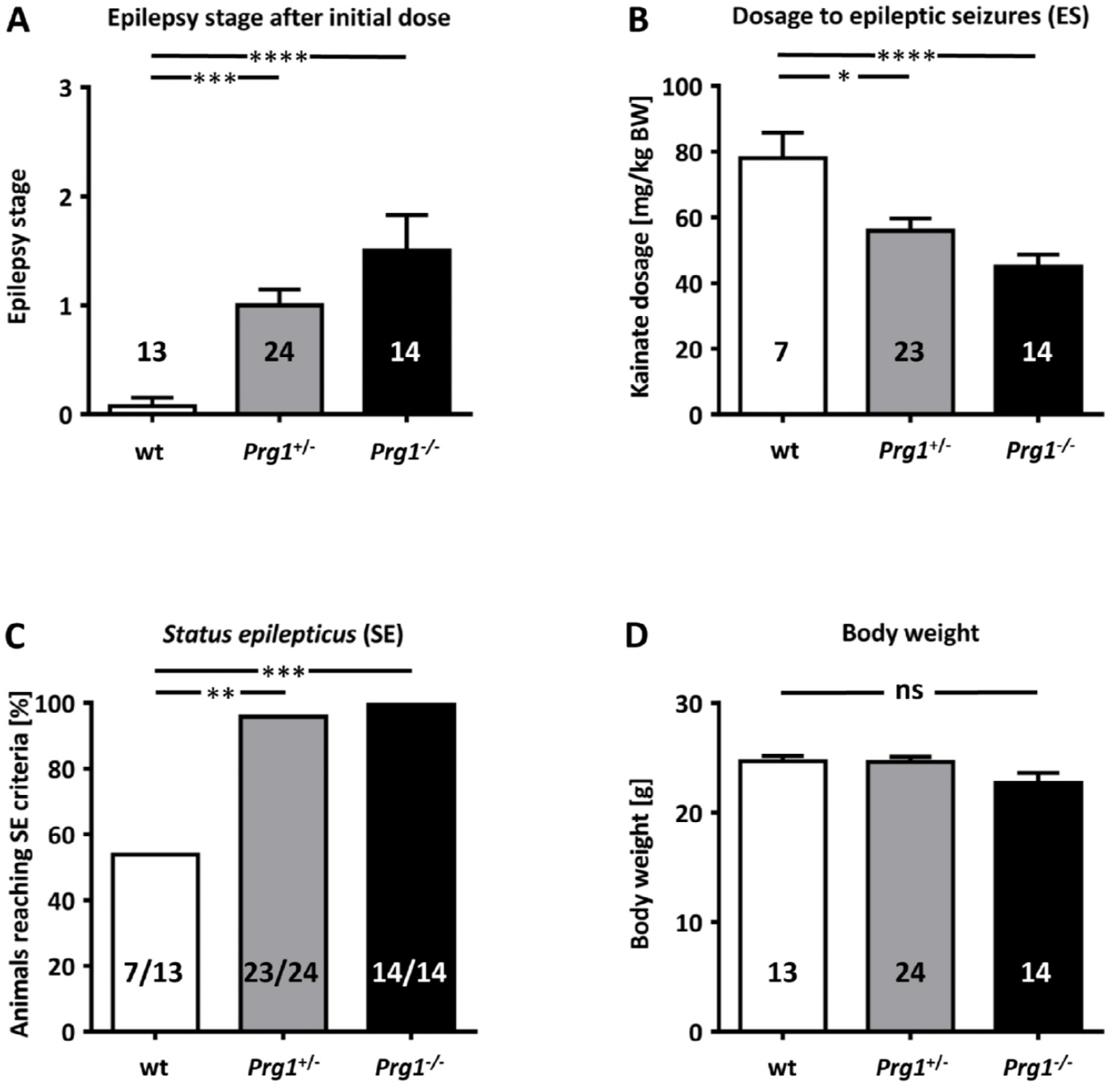

Knierim *et al*., Figure 3

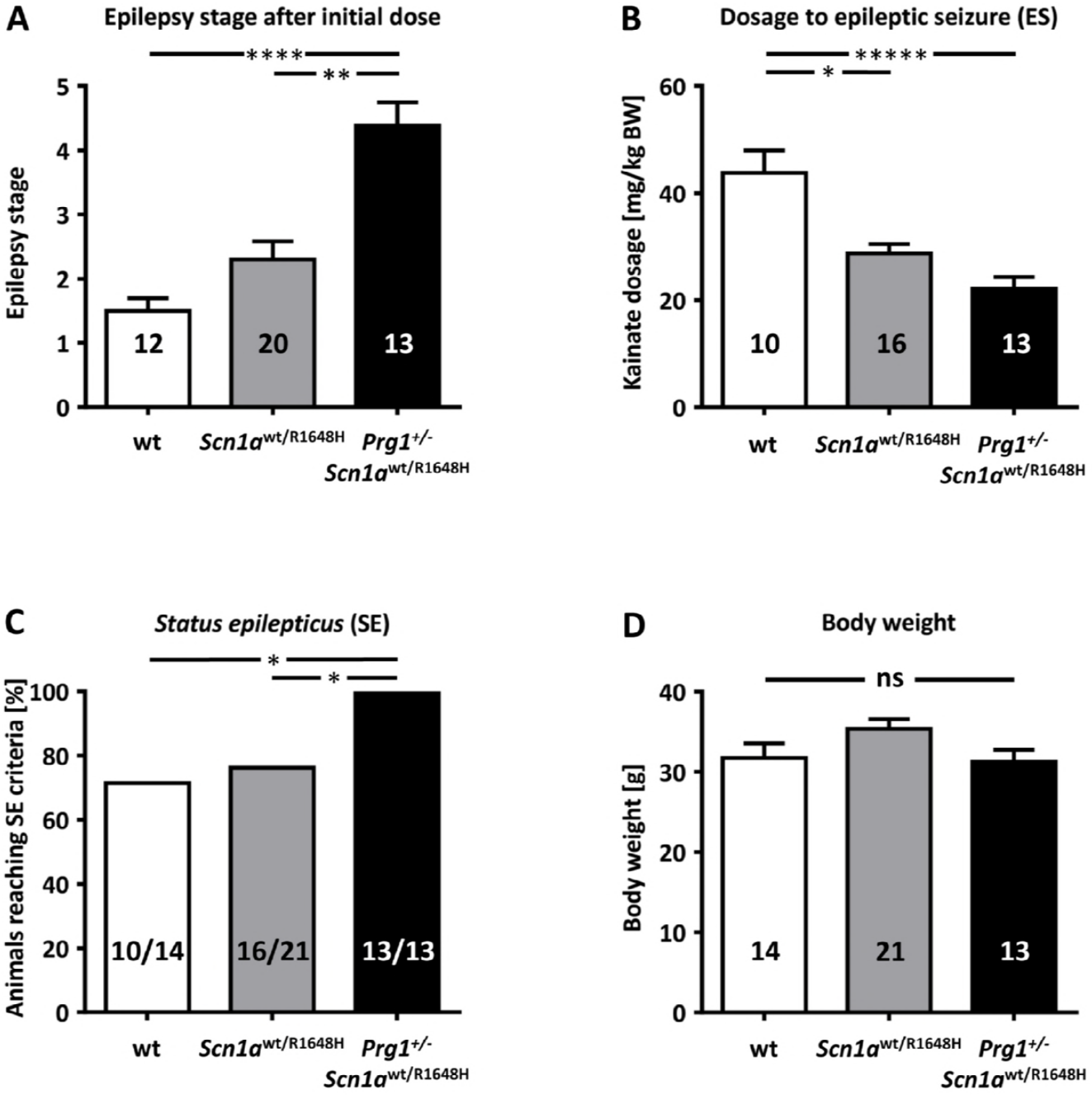

Knierim *et al.*, Figure 4

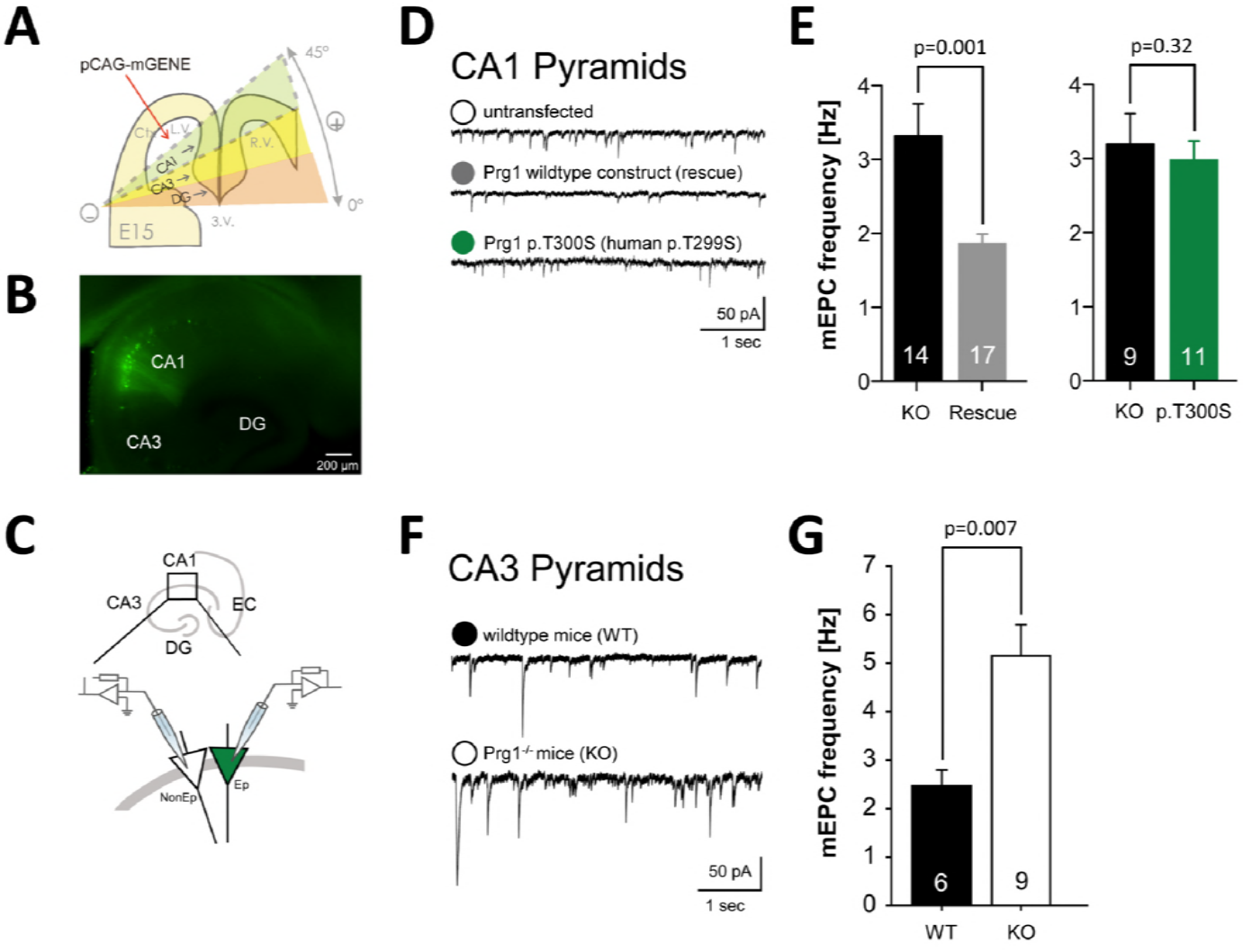

Knierim *et al.*, Figure 5

Supplementary table 01: Panel of 350 genes that are known to be associated with a Mendelian trait that involves cerebral seizures (sorted in alphabetical order). The chromosomal positions refer to genome build GRCh37.p11 (hg19/Ensembl 72).

GENE	DESCRIPTION	CHR	POS START	POS END
ABCC8	ATP-binding cassette, sub-family C (CFTR/MRP), member 8	11	17.498.449	17.414.432
ACY1	aminoacylase 1	3	52.023.218	52.017.300
ADCK3	aarF domain containing kinase 3	1	227.175.246	227.084.589
ADSL	adenylosuccinate lyase	22	40.762.577	40.742.504
AGA	aspartylglucosaminidase	4	178.363.657	178.351.928
AHI1	Abelson helper integration site 1	6	135.818.903	135.604.670
ALDH4A1	aldehyde dehydrogenase 4 family, member A1	1	19.229.293	19.197.924
ALDH5A1	aldehyde dehydrogenase 5 family, member A1	6	24.537.435	24.495.197
ALDH7A1	aldehyde dehydrogenase 7 family, member A1	5	125.931.104	125.877.533
ALG1	ALG1, chitobiosyldiphosphodolichol beta-mannosyltransferase	16	5.137.380	5.121.810
ALG12	ALG12, alpha-1,6-mannosyltransferase	22	50.312.106	50.296.852
ALG13	ALG13, UDP-N-acetylglucosaminyltransferase subunit	23	110924346	111003877
ALG2	ALG2, alpha-1,3/1,6-mannosyltransferase	9	101.984.246	101.978.707
ALG3	ALG3, alpha-1,3- mannosyltransferase	3	183.967.313	183.960.117
ALG6	ALG6, alpha-1,3-glucosyltransferase	1	63.904.233	63.833.261
ALG8	ALG8, alpha-1,3-glucosyltransferase	11	77.850.699	77.811.988
ALG9	ALG9, alpha-1,2-mannosyltransferase	11	111.742.305	111.652.919
AMT	aminomethyltransferase	3	49.460.111	49.454.211
APTX	aprataxin	9	33.001.639	32.972.604
ARFGEF2	ADP-ribosylation factor guanine nucleotide-exchange factor 2 (brefeldin A-inhibited)	20	47.653.230	47.538.250
ARG1	arginase 1	6	131.905.472	131.894.344
ARHGEF9	Cdc42 guanine nucleotide exchange factor (GEF) 9	23	63.005.426	62.854.847
ARL13B	ADP-ribosylation factor-like 13B	3	93.774.522	93.698.983
ARSA	arylsulfatase A	22	51.066.601	51.061.182
ARSB	arylsulfatase B	5	78.282.357	78.073.032
ARX	aristaless related homeobox	23	25.034.065	25.021.811
ASPA	aspartoacylase	17	3.402.700	3.377.404
ASPM	asp (abnormal spindle) homolog, microcephaly associated (Drosophila)	1	197.115.824	197.053.257
ATIC	5-aminoimidazole-4-carboxamide ribonucleotide formyltransferase/IMP cyclohydrolase	2	216.214.496	216.176.679
ATP1A2	ATPase, Na+/K+ transporting, alpha 2 polypeptide	1	160.113.381	160.085.520
ATP2A2	ATPase, Ca++ transporting, cardiac muscle, slow twitch 2	12	110.788.898	110.719.032
ATP6AP2	ATPase, H+ transporting, lysosomal accessory protein 2	23	40.465.889	40.440.141
ATP6V0A2	ATPase, H+ transporting, lysosomal V0 subunit a2	12	124.246.302	124.196.865
ATPAF2	ATP synthase mitochondrial F1 complex assembly factor 2	17	17.942.483	17.921.334
ATR	ataxia telangiectasia and Rad3 related	3	142.297.668	142.168.077
ATRX	alpha thalassemia/mental retardation syndrome X-linked	23	77.041.755	76.760.356
B4GALT1	UDP-Gal:betaGlcNAc beta 1,4- galactosyltransferase, polypeptide 1	9	33.167.356	33.110.636
BCKDK	branched chain ketoacid dehydrogenase kinase	16	31.124.112	31.119.615
BCS1L	BC1 (ubiquinol-cytochrome c reductase) synthesis-like	2	219.528.166	219.524.379
BOLA3	bolA family member 3	2	74.375.039	74.362.528
BRAF	v-raf murine sarcoma viral oncogene homolog B	7	140.624.564	140.415.749
BRD2	bromodomain containing 2	6	32.949.282	32.936.437
BTD	biotinidase	3	15.689.147	15.642.864
BUB1B	BUB1 mitotic checkpoint serine/threonine kinase B	15	40.513.337	40.453.210
C12orf65	chromosome 12 open reading frame 65	12	123.742.651	123.717.844
CACNA1A	calcium channel, voltage-dependent, P/Q type, alpha 1A subunit	19	13.617.274	13.317.256
CACNA1H	calcium channel, voltage-dependent, T type, alpha 1H subunit	16	1.271.772	1.203.241
CACNA2D2	calcium channel, voltage-dependent, alpha 2/delta subunit 2	3	50.540.892	50.400.230
CACNB4	calcium channel, voltage-dependent, beta 4 subunit	2	152.955.593	152.689.285
CARS2	cysteinyl-tRNA synthetase 2, mitochondrial (putative)	13	111293757	111358480
CASK	calcium/calmodulin-dependent serine protein kinase (MAGUK family)	23	41.782.415	41.374.187
CASR	calcium-sensing receptor	3	122.005.350	121.902.530
CBL	Cbl proto-oncogene, E3 ubiquitin protein ligase	11	119.178.859	119.076.986
CC2D2A	coiled-coil and C2 domain containing 2A	4	15.603.594	15.471.489
CCDC88C	coiled-coil domain containing 88C	14	91.884.188	91.737.667
CDK5RAP2	CDK5 regulatory subunit associated protein 2	9	123.342.448	123.151.147
CDKL5	cyclin-dependent kinase-like 5	23	18.671.749	18.443.725
CENPJ	centromere protein J	13	25.497.027	25.456.412
CEP152	centrosomal protein 152kDa	15	49.104.092	49.030.135
CEP290	centrosomal protein 290kDa	12	88.535.993	88.442.790
CHD2	chromodomain helicase DNA binding protein 2	15	93442286	93571237
CHRNA2	cholinergic receptor, nicotinic, alpha 2 (neuronal)	8	27.336.813	27.317.278
CHRNA4	cholinergic receptor, nicotinic, alpha 4 (neuronal)	20	62.009.487	61.974.662
CHRNB2	cholinergic receptor, nicotinic, beta 2 (neuronal)	1	154.552.354	154.540.257
CLCN2	chloride channel, voltage-sensitive 2	3	184.079.439	184.063.973
CLCNKA	chloride channel, voltage-sensitive Ka	1	16.360.548	16.348.486
CLCNKB	chloride channel, voltage-sensitive Kb	1	16.383.821	16.370.231
CLN3	ceroid-lipofuscinosis, neuronal 3	16	28.505.897	28.488.600
CLN5	ceroid-lipofuscinosis, neuronal 5	13	77.576.652	77.566.059
CLN6	ceroid-lipofuscinosis, neuronal 6, late infantile, variant	15	68.522.081	68.499.330
CLN8	ceroid-lipofuscinosis, neuronal 8 (epilepsy, progressive with mental retardation)	8	1.734.736	1.703.944
CNTNAP2	contactin associated protein-like 2	7	148.118.090	145.813.453
COG1	component of oligomeric golgi complex 1	17	71.204.646	71.189.070
COG7	component of oligomeric golgi complex 7	16	23.464.583	23.399.814

GENE	DESCRIPTION	CHR	POS START	POS END
COG8	component of oligomeric golgi complex 8	16	69.373.526	69.362.524
COL18A1	collagen, type XVIII, alpha 1	21	46.933.634	46.825.058
COL4A1	collagen, type IV, alpha 1	13	110.959.496	110.801.310
COQ2	coenzyme Q2 4-hydroxybenzoate polyprenyltransferase	4	84.206.067	84.184.972
COQ9	coenzyme Q9	16	57.495.187	57.481.337
COX10	cytochrome c oxidase assembly homolog 10 (yeast)	17	14.111.996	13.972.719
COX15	cytochrome c oxidase assembly homolog 15 (yeast)	10	101.492.423	101.455.886
CPT2	carnitine palmitoyltransferase 2	1	53.679.869	53.662.101
CSTB	cystatin B (stefin B)	21	45.196.256	45.193.546
CTSA	cathepsin A	20	44.527.459	44.519.591
CTSD	cathepsin D	11	1.785.222	1.773.982
CUL4B	cullin 4B	23	119.709.684	119.658.444
DCX	doublecortin	23	110.655.460	110.537.007
DEPDC5	DEP domain containing 5	22	32.303.020	32.149.937
DLD	dihydrolipoamide dehydrogenase	7	107.561.643	107.531.586
DNAJC5	DnaJ (Hsp40) homolog, subfamily C, member 5	20	62.567.384	62.526.455
DOLK	dolichol kinase	9	131.710.012	131.707.809
DPAGT1	dolichyl-phosphate (UDP-N-acetylglucosamine) N-acetylglucosaminephosphotransferase 1 (GlcNAc-1-P transferase)	11	118.973.124	118.967.213
DPM1	dolichyl-phosphate mannosyltransferase polypeptide 1, catalytic subunit	20	49.575.081	49.551.404
DPM3	dolichyl-phosphate mannosyltransferase polypeptide 3	1	155.112.996	155.112.367
DPYD	dihydropyrimidine dehydrogenase	1	98.386.615	97.543.299
EFHC1	EF-hand domain (C-terminal) containing 1	6	52.360.583	52.284.994
EIF2B1	eukaryotic translation initiation factor 2B, subunit 1 alpha, 26kDa	12	124.118.323	124.105.570
EIF2B2	eukaryotic translation initiation factor 2B, subunit 2 beta, 39kDa	14	75.476.294	75.469.612
EIF2B3	eukaryotic translation initiation factor 2B, subunit 3 gamma, 58kDa	1	45.452.394	45.316.194
EIF2B4	eukaryotic translation initiation factor 2B, subunit 4 delta, 67kDa	2	27.593.324	27.587.219
EIF2B5	eukaryotic translation initiation factor 2B, subunit 5 epsilon, 82kDa	3	183.863.099	183.852.810
EMX2	empty spiracles homeobox 2	10	119.309.057	119.301.956
EOMES	eomesodermin	3	27.764.206	27.757.440
EPM2A	epilepsy, progressive myoclonus type 2A, Lafora disease (laforin)	6	146.057.128	145.946.440
ETFA	electron-transfer-flavoprotein, alpha polypeptide	15	76.603.810	76.508.628
ETFB	electron-transfer-flavoprotein, beta polypeptide	19	51.869.672	51.848.409
ETFDH	electron-transferring-flavoprotein dehydrogenase	4	159.629.842	159.593.277
FGD1	FYVE, RhoGEF and PH domain containing 1	23	54.522.599	54.471.887
FGF8	fibroblast growth factor 8 (androgen-induced)	10	103.540.126	103.529.887
FGFR3	fibroblast growth factor receptor 3	4	1.810.599	1.795.039
FH	fumarate hydratase	1	241.683.085	241.660.857
FKRP	fukutin related protein	19	47.261.832	47.249.303
FKTN	fukutin	9	108.403.399	108.320.411
FLNA	filamin A, alpha	23	153.603.006	153.576.900
FOLR1	folate receptor 1 (adult)	11	71.907.367	71.900.602
FOXG1	forkhead box G1	14	29.239.483	29.236.278
FUCA1	fucosidase, alpha-L- 1, tissue	1	24.194.859	24.171.567
GABRA1	gamma-aminobutyric acid (GABA) A receptor, alpha 1	5	161.326.965	161.274.197
GABRB3	gamma-aminobutyric acid (GABA) A receptor, beta 3	15	27.018.935	26.788.693
GABRD	gamma-aminobutyric acid (GABA) A receptor, delta	1	1.962.192	1.950.768
GABRG2	gamma-aminobutyric acid (GABA) A receptor, gamma 2	5	161.582.545	161.494.648
GALC	galactosylceramidase	14	88.460.009	88.304.164
GALNS	galactosamine (N-acetyl)-6-sulfate sulfatase	16	88.923.374	88.880.142
GAMT	guanidinoacetate N-methyltransferase	19	1.401.569	1.397.025
GCDH	glutaryl-CoA dehydrogenase	19	13.010.813	13.001.943
GCSH	glycine cleavage system protein H (aminomethyl carrier)	16	81.129.980	81.115.552
GFAP	glial fibrillary acidic protein	17	42.992.920	42.982.994
GLB1	galactosidase, beta 1	3	33.138.694	33.038.100
GLDC	glycine dehydrogenase (decarboxylating)	9	6.645.692	6.532.464
GLI2	GLI family zinc finger 2	2	121.750.229	121.493.441
GLI3	GLI family zinc finger 3	7	42.277.469	42.000.547
GLRA1	glycine receptor, alpha 1	5	151.304.397	151.202.074
GLRB	glycine receptor, beta	4	158.093.251	157.997.277
GLUL	glutamate-ammonia ligase	1	182.361.341	182.350.839
GNE	glucosamine (UDP-N-acetyl)-2-epimerase/N-acetylmannosamine kinase	9	36.277.053	36.214.438
GNPTAB	N-acetylglucosamine-1-phosphate transferase, alpha and beta subunits	12	102.224.645	102.139.275
GNPTG	N-acetylglucosamine-1-phosphate transferase, gamma subunit	16	1.413.352	1.401.900
GNS	glucosamine (N-acetyl)-6-sulfatase	12	65.153.226	65.107.222
GPC3	glypican 3	23	133.119.673	132.669.773
GPHN	gephyrin	14	67.648.525	66.974.125
GPR56	G protein-coupled receptor 56	16	57.698.944	57.653.442
GPR98	G protein-coupled receptor 98	5	90.460.254	89.854.617
GRIA3	glutamate receptor, ionotropic, AMPA 3	23	122.624.766	122.317.996
GRIN1	glutamate receptor, ionotropic, N-methyl D-aspartate 1	9	140033609	140063214
GRIN2A	glutamate receptor, ionotropic, N-methyl D-aspartate 2A	16	10.276.611	9.847.265
GRIN2B	glutamate receptor, ionotropic, N-methyl D-aspartate 2B	12	14.133.022	13.713.684
GUSB	glucuronidase, beta	7	65.447.301	65.425.671
HCN1	hyperpolarization activated cyclic nucleotide-gated potassium channel 1	5	45255052	45696220
HEXA	hexosaminidase A (alpha polypeptide)	15	72.669.474	72.635.778
HEXB	hexosaminidase B (beta polypeptide)	5	74.017.113	73.935.547
HGSNAT	heparan-alpha-glucosaminide N-acetyltransferase	8	43.057.970	42.995.592

GENE	DESCRIPTION	CHR	POS START	POS END
HPD	4-hydroxyphenylpyruvate dioxygenase	12	122.326.517	122.277.433
HRAS	Harvey rat sarcoma viral oncogene homolog	11	535.561	532.242
HSD17B10	hydroxysteroid (17-beta) dehydrogenase 10	23	53.461.323	53.458.206
HYAL1	hyaluronoglucosaminidase 1	3	50.349.812	50.337.320
IDS	iduronate 2-sulfatase	23	148.586.884	148.560.295
IDUA	iduronidase, alpha-L-	4	998.317	980.785
INPP5E	inositol polyphosphate-5-phosphatase, 72 kDa	9	139.334.305	139.323.067
KAT6B	K(lysine) acetyltransferase 6B	10	76.792.380	76.584.685
KCNA1	potassium voltage-gated channel, shaker-related subfamily, member 1 (episodic ataxia with myokymia)	12	5.027.422	5.019.073
KCNC1	potassium voltage-gated channel, Shaw-related subfamily, member 1	11	17757495	17804602
KCNJ1	potassium inwardly-rectifying channel, subfamily J, member 1	11	128.737.268	128.707.909
KCNJ10	potassium inwardly-rectifying channel, subfamily J, member 10	1	160.040.051	160.007.257
KCNMA1	potassium large conductance calcium-activated channel, subfamily M, alpha member 1	10	79.397.577	78.629.359
KCNQ2	potassium voltage-gated channel, KQT-like subfamily, member 2	20	62.103.993	62.031.561
KCNQ3	potassium voltage-gated channel, KQT-like subfamily, member 3	8	133.493.004	133.133.105
KCNT1	potassium channel, subfamily T, member 1	9	138.684.993	138.594.031
KCTD7	potassium channel tetramerization domain containing 7	7	66.113.964	66.093.868
KDM5C	lysine (K)-specific demethylase 5C	23	53.254.604	53.220.503
KIAA1279	KIAA1279	10	70.776.739	70.748.477
KRAS	Kirsten rat sarcoma viral oncogene homolog	12	25.403.870	25.358.180
L2HGDH	L-2-hydroxyglutarate dehydrogenase	14	50.778.947	50.704.285
LAMA2	laminin, alpha 2	6	129.837.711	129.204.286
LARGE	like-glycosyltransferase	22	34.316.464	33.668.509
LBR	lamin B receptor	1	225.616.557	225.589.204
LGI1	leucine-rich, glioma inactivated 1	10	95.557.916	95.517.566
LIG4	ligase IV, DNA, ATP-dependent	13	108.870.716	108.859.790
LRPPRC	leucine-rich pentatricopeptide repeat containing	2	44.223.144	44.113.363
MAGI2	membrane associated guanylate kinase, WW and PDZ domain containing 2	7	79.083.121	77.646.374
MAP2K1	mitogen-activated protein kinase kinase 1	15	66.783.882	66.679.182
MAP2K2	mitogen-activated protein kinase kinase 2	19	4.124.126	4.090.319
MAPK10	mitogen-activated protein kinase 10	4	87.374.283	86.933.452
MBD5	methyl-CpG binding domain protein 5	2	149.271.046	148.778.580
MCOLN1	mucolipin 1	19	7.598.895	7.587.496
MCPH1	microcephalin 1	8	6.501.140	6.264.113
ME2	malic enzyme 2, NAD(+)-dependent, mitochondrial	18	48.476.165	48.405.432
MECP2	methyl CpG binding protein 2 (Rett syndrome)	23	153.363.188	153.287.025
MED12	mediator complex subunit 12	23	70.362.304	70.338.406
MED17	mediator complex subunit 17	11	93.546.496	93.517.405
MFSD8	major facilitator superfamily domain containing 8	4	128.887.185	128.838.960
MGAT2	mannosyl (alpha-1,6-)-glycoprotein beta-1,2-N-acetylglucosaminyltransferase	14	50.090.199	50.087.460
MLC1	megalencephalic leukoencephalopathy with subcortical cysts 1	22	50.524.358	50.497.820
MOCS1	molybdenum cofactor synthesis 1	6	39.902.290	39.872.034
MOCS2	molybdenum cofactor synthesis 2	5	52.405.602	52.391.509
MOGS	mannosyl-oligosaccharide glucosidase	2	74.692.537	74.688.184
MPDU1	mannose-P-dolichol utilization defect 1	17	7.491.530	7.486.965
MPI	mannose phosphate isomerase	15	75.190.581	75.182.377
MTHFR	methylenetetrahydrofolate reductase (NAD(P)H)	1	11.866.160	11.845.787
NAGLU	N-acetylglucosaminidase, alpha	17	40.696.467	40.687.951
NDUFA2	NADH dehydrogenase (ubiquinone) 1 alpha subcomplex, 2, 8kDa	5	140.027.370	140.024.948
NDUFAF6	NADH dehydrogenase (ubiquinone) complex I, assembly factor 6	8	96.115.685	96.037.209
NDUFS1	NADH dehydrogenase (ubiquinone) Fe-S protein 1, 75kDa (NADH-coenzyme Q reductase)	2	207.024.243	206.987.803
NDUFS3	NADH dehydrogenase (ubiquinone) Fe-S protein 3, 30kDa (NADH-coenzyme Q reductase)	11	47.606.115	47.600.562
NDUFS4	NADH dehydrogenase (ubiquinone) Fe-S protein 4, 18kDa (NADH-coenzyme Q reductase)	5	52.979.171	52.856.464
NDUFS7	NADH dehydrogenase (ubiquinone) Fe-S protein 7, 20kDa (NADH-coenzyme Q reductase)	19	1.395.588	1.383.526
NDUFS8	NADH dehydrogenase (ubiquinone) Fe-S protein 8, 23kDa (NADH-coenzyme Q reductase)	11	67.804.114	67.798.084
NDUFV1	NADH dehydrogenase (ubiquinone) flavoprotein 1, 51kDa	11	67.380.012	67.374.323
NEU1	sialidase 1 (lysosomal sialidase)	6	31.830.709	31.826.829
NF1	neurofibromin 1	17	29.704.695	29.421.945
NHEJ1	nonhomologous end-joining factor 1	2	220.025.587	219.940.046
NHLRC1	NHL repeat containing E3 ubiquitin protein ligase 1	6	18.122.851	18.120.718
NIPBL	Nipped-B homolog (Drosophila)	5	37.065.926	36.876.861
NKAIN2	Na+/K+ transporting ATPase interacting 2	6	125.146.786	124.124.991
NOTCH3	notch 3	19	15.311.792	15.270.444
NPC1	Niemann-Pick disease, type C1	18	21.166.581	21.086.148
NPC2	Niemann-Pick disease, type C2	14	74.960.084	74.942.900
NPHP1	nephronophthisis 1 (juvenile)	2	110.962.639	110.880.913
NRAS	neuroblastoma RAS viral (v-ras) oncogene homolog	1	115.259.515	115.247.085
NRXN1	neurexin 1	2	51.259.674	50.145.643
OFD1	oral-facial-digital syndrome 1	23	13.787.480	13.733.549
OPHN1	oligophrenin 1	23	67.653.369	67.262.186
PAFAH1B1	platelet-activating factor acetylhydrolase 1b, regulatory subunit 1 (45kDa)	17	2.588.909	2.496.923
PAK3	p21 protein (Cdc42/Rac)-activated kinase 3	23	110.470.590	110.187.513
PANK2	pantothenate kinase 2	20	3.904.538	3.869.486
PAX6	paired box 6	11	31.839.509	31.806.340
PC	pyruvate carboxylase	11	66.725.847	66.615.993
PCDH19	protocadherin 19	23	99.665.271	99.546.642
PCNT	pericentrin	21	47.865.682	47.743.976

GENE	DESCRIPTION	CHR	POS START	POS END
PDHA1	pyruvate dehydrogenase (lipoamide) alpha 1	23	19.379.825	19.362.011
PDSS1	prenyl (decaprenyl) diphosphate synthase, subunit 1	10	27.035.727	26.986.353
PDSS2	prenyl (decaprenyl) diphosphate synthase, subunit 2	6	107.780.779	107.473.761
PEX1	peroxisomal biogenesis factor 1	7	92.157.845	92.116.337
PEX12	peroxisomal biogenesis factor 12	17	33.905.656	33.901.814
PEX14	peroxisomal biogenesis factor 14	1	10.690.815	10.535.003
PEX2	peroxisomal biogenesis factor 2	8	77.913.280	77.892.494
PEX26	peroxisomal biogenesis factor 26	22	18.573.797	18.560.686
PEX3	peroxisomal biogenesis factor 3	6	143.811.753	143.771.918
PEX5	peroxisomal biogenesis factor 5	12	7.371.170	7.341.759
PEX6	peroxisomal biogenesis factor 6	6	42.946.981	42.931.611
PEX7	peroxisomal biogenesis factor 7	6	137.235.072	137.143.702
PGK1	phosphoglycerate kinase 1	23	77.382.324	77.359.666
PHF6	PHD finger protein 6	23	133.562.822	133.507.324
PHGDH	phosphoglycerate dehydrogenase	1	120.286.849	120.254.419
PIGV	phosphatidylinositol glycan anchor biosynthesis, class V	1	27.124.894	27.113.739
PLA2G6	phospholipase A2, group VI (cytosolic, calcium-independent)	22	38.577.857	38.507.502
PLCB1	phospholipase C, beta 1 (phosphoinositide-specific)	20	8.865.547	8.112.912
PLP1	proteolipid protein 1	23	103.047.548	103.031.439
PMM2	phosphomannomutase 2	16	8.943.194	8.891.670
PNKP	polynucleotide kinase 3'-phosphatase	19	50.370.840	50.364.460
PNPO	pyridoxamine 5'-phosphate oxidase	17	46.026.674	46.018.889
POLG	polymerase (DNA directed), gamma	15	89.878.026	89.859.536
POMGNT1	protein O-linked mannose N-acetylglucosaminyltransferase 1 (beta 1,2-)	1	46.685.977	46.654.353
POMT1	protein-O-mannosyltransferase 1	9	134.399.193	134.378.282
POMT2	protein-O-mannosyltransferase 2	14	77.787.225	77.741.299
PPT1	palmitoyl-protein thioesterase 1	1	40.563.142	40.538.382
PQBP1	polyglutamine binding protein 1	23	48.760.422	48.755.160
PRICKLE1	prickle homolog 1 (Drosophila)	12	42.983.572	42.852.140
PRICKLE2	prickle homolog 2 (Drosophila)	3	64.253.859	64.079.526
PRODH	proline dehydrogenase (oxidase) 1	22	18.924.066	18.900.206
PRRT2	proline-rich transmembrane protein 2	16	29.827.202	29.823.409
PSAP	prosaposin	10	73.611.082	73.576.055
PTCH1	patched 1	9	98.279.247	98.205.264
PTPN11	protein tyrosine phosphatase, non-receptor type 11	12	112.947.717	112.856.536
QDPR	quinoid dihydropteridine reductase	4	17.513.857	17.488.016
RAB39B	RAB39B, member RAS oncogene family	23	154.493.852	154.487.526
RAB3GAP1	RAB3 GTPase activating protein subunit 1 (catalytic)	2	135.928.280	135.809.835
RAF1	v-raf-1 murine leukemia viral oncogene homolog 1	3	12.705.700	12.625.100
RAI1	retinoic acid induced 1	17	17.714.767	17.584.787
RARS2	arginyl-tRNA synthetase 2, mitochondrial	6	88.299.735	88.223.656
RBFOX1	RNA binding protein, fox-1 homolog (C. elegans) 1	16	7.763.342	5.289.469
RELN	reelin	7	103.629.963	103.112.231
RFT1	RFT1 homolog (S. cerevisiae)	3	53.164.480	53.122.499
RNASEH2A	ribonuclease H2, subunit A	19	12.924.462	12.912.863
RNASEH2B	ribonuclease H2, subunit B	13	51.544.596	51.483.814
RNASEH2C	ribonuclease H2, subunit C	11	65.488.409	65.485.144
RPGRIP1L	RPGRIP1-like	16	53.737.771	53.633.818
SAMHD1	SAM domain and HD domain 1	20	35.580.246	35.519.285
SCARB2	scavenger receptor class B, member 2	4	77.135.052	77.079.890
SCN1A	sodium channel, voltage-gated, type I, alpha subunit	2	167.005.642	166.845.670
SCN1B	sodium channel, voltage-gated, type I, beta subunit	19	35.531.353	35.521.555
SCN2A	sodium channel, voltage-gated, type II, alpha subunit	2	166.248.820	165.986.659
SCN8A	sodium channel, voltage gated, type VIII, alpha subunit	12	52.206.648	51.984.050
SCN9A	sodium channel, voltage-gated, type IX, alpha subunit	2	167.232.497	167.051.695
SCO2	SCO2 cytochrome c oxidase assembly protein	22	50.964.868	50.961.997
SDHA	succinate dehydrogenase complex, subunit A, flavoprotein (Fp)	5	256.815	218.338
SERPINI1	serpin peptidase inhibitor, clade I (neuroserpin), member 1	3	167.543.357	167.453.432
SETBP1	SET binding protein 1	18	42.648.475	42.258.849
SGSH	N-sulfoglucosamine sulfohydrolase	17	78.194.199	78.180.515
SHH	sonic hedgehog	7	155.604.967	155.595.558
SHOC2	soc-2 suppressor of clear homolog (C. elegans)	10	112.773.425	112.679.301
SIX3	SIX homeobox 3	2	45.173.216	45.169.037
SLC17A5	solute carrier family 17 (acidic sugar transporter), member 5	6	74.363.737	74.303.102
SLC19A3	solute carrier family 19 (thiamine transporter), member 3	2	228.582.814	228.549.926
SLC25A15	solute carrier family 25 (mitochondrial carrier; ornithine transporter) member 15	13	41.386.601	41.363.547
SLC25A19	solute carrier family 25 (mitochondrial thiamine pyrophosphate carrier), member 19	17	73.285.530	73.269.061
SLC25A22	solute carrier family 25 (mitochondrial carrier: glutamate), member 22	11	798.269	790.475
SLC2A1	solute carrier family 2 (facilitated glucose transporter), member 1	1	43.424.847	43.391.046
SLC35A1	solute carrier family 35 (CMP-sialic acid transporter), member A1	6	88.222.057	88.182.637
SLC35C1	solute carrier family 35 (GDP-fucose transporter), member C1	11	45.834.568	45.825.623
SLC46A1	solute carrier family 46 (folate transporter), member 1	17	26.733.230	26.721.661
SLC4A10	solute carrier family 4, sodium bicarbonate transporter, member 10	2	162.841.786	162.480.699
SLC6A5	solute carrier family 6 (neurotransmitter transporter), member 5	11	20.676.610	20.620.946
SLC6A8	solute carrier family 6 (neurotransmitter transporter), member 8	23	152.962.048	152.953.752
SLC9A6	solute carrier family 9, subfamily A (NHE6, cation proton antiporter 6), member 6	23	135.129.428	135.067.583
SMC1A	structural maintenance of chromosomes 1A	23	53.449.677	53.401.070

GENE	DESCRIPTION	CHR	POS START	POS END
SMC3	structural maintenance of chromosomes 3	10	112.364.392	112.327.449
SMPD1	sphingomyelin phosphodiesterase 1, acid lysosomal	11	6.416.228	6.411.644
SMS	spermine synthase	23	22.025.798	21.958.691
SNAP29	synaptosomal-associated protein, 29kDa	22	21.245.502	21.213.292
SOS1	son of sevenless homolog 1 (Drosophila)	2	39.347.686	39.208.690
SPRED1	sprouty-related, EVH1 domain containing 1	15	38.649.450	38.544.925
SPTAN1	spectrin, alpha, non-erythrocytic 1	9	131.395.944	131.314.837
SRGAP2	SLIT-ROBO Rho GTPase activating protein 2	1	206.135.657	206.135.293
SRGAP2	SLIT-ROBO Rho GTPase activating protein 2	1	206.637.783	206.516.197
SRPX2	sushi-repeat containing protein, X-linked 2	23	99.926.296	99.899.163
STIL	SCL/TAL1 interrupting locus	1	47.779.819	47.715.811
STX1B	syntaxin 1B	16	31000577	31021829
STXBP1	syntaxin binding protein 1	9	130.454.995	130.374.486
SUMF1	sulfatase modifying factor 1	3	4.508.966	4.402.829
SUOX	sulfite oxidase	12	56.399.309	56.391.043
SURF1	surfeit 1	9	136.223.361	136.218.660
SYNGAP1	synaptic Ras GTPase activating protein 1	6	33.421.466	33.387.847
SYP	synaptophysin	23	49.056.661	49.044.263
TACO1	translational activator of mitochondrially encoded cytochrome c oxidase I	17	61.685.725	61.678.231
TBC1D24	TBC1 domain family, member 24	16	2.555.734	2.525.146
TBCE	tubulin folding cofactor E	1	235.612.280	235.530.728
TBX1	T-box 1	22	19.771.116	19.744.226
TCF4	transcription factor 4	18	53.303.252	52.889.562
TGIF1	TGFB-induced factor homeobox 1	18	3.458.409	3.411.925
TMEM216	transmembrane protein 216	11	61.166.335	61.159.832
TMEM67	transmembrane protein 67	8	94.831.462	94.767.072
TMEM70	transmembrane protein 70	8	74.895.018	74.888.377
TPP1	tripeptidyl peptidase I	11	6.640.692	6.633.997
TREX1	three prime repair exonuclease 1	3	48.509.044	48.506.919
TSC1	tuberous sclerosis 1	9	135.820.094	135.766.735
TSC2	tuberous sclerosis 2	16	2.138.713	2.097.472
TSEN2	TSEN2 tRNA splicing endonuclease subunit	3	12.580.672	12.517.748
TSEN34	TSEN34 tRNA splicing endonuclease subunit	19	54.698.394	54.694.112
TSEN54	TSEN54 tRNA splicing endonuclease subunit	17	73.520.821	73.512.609
TUBA1A	tubulin, alpha 1a	12	49.583.107	49.578.578
TUBA8	tubulin, alpha 8	22	18.614.498	18.593.453
TUBB2B	tubulin, beta 2B class IIb	6	3.227.968	3.224.495
UBE3A	ubiquitin protein ligase E3A	15	25.684.190	25.582.394
VDAC1	voltage-dependent anion channel 1	5	133.341.300	133.307.566
VPS13A	vacuolar protein sorting 13 homolog A (S. cerevisiae)	9	80.032.399	79.792.269
VPS13B	vacuolar protein sorting 13 homolog B (yeast)	8	100.890.447	100.025.299
VRK1	vaccinia related kinase 1	14	97.347.951	97.263.684
WDR62	WD repeat domain 62	19	36.596.012	36.545.783
ZEB2	zinc finger E-box binding homeobox 2	2	145.277.958	145.141.942
ZIC2	Zic family member 2	13	100.639.019	100.634.026

GENE	GENE NAME	OMIM	MOI	OMIM DISEASE NAME	DISEASE EXCLUDED IN THE INDEX PATIENT (II:2) BY	ENSEMBL TRANSCRIPT	CHR	POS [HG19]	VARIANT	AAE	COVERAGE [fold]	VARIANT FREQUENCY [%]	dbSNP	MAJOR ALLELE HOMO *	HET *	MINOR ALLELE HOMO *	ExAC SERVER: VARIANTS PER ALLELES (TOTAL)
GLI2	GLI family zinc finger 2	#610829	AD	Holoprosencephaly type 9	Absence of structural abnormalities in the brain of the index patient	ENST00000361492	2	121.748.048	G>A	D1520N	171	46	rs114814747	1083	11	0	1.220 / 121.386
SCN1A	Sodium channel, neuro-nal type I, alpha-subunit	#604403	AD	Generalized epilepsy with febrile seizures plus, type 2 (GEFSP2)		ENST00000409050	2	166.901.593	T>C	N541S	305	50	.				0 / 121.380
ACY1	Aminoacylase 1	#609924	AR	Aminoacylase 1 deficiency	Absence of hearing loss and dysmorphic features, normal amino acid excretion into the urine	ENST00000458031	3	52.023.042	G>A	R483H	222	50	rs121912701	1087	7	0	482 / 120.860
PEX6	Peroxisomal biogenesis factor 6	#614862	AR	Peroxysome biogenesis disorder type 4b	Absence of clinical features reminiscent of Zellweger syndrome	ENST00000304611	6	42.932.200	GGC>TGT	P939Q	24	46	rs1129187				46.985 / 120.122
CDK5RAP2	CDK5 regulatory subunit associated protein 2	#604804	AR	Microphephaly type 3	Absence of microcephaly, hearing loss, and of structural abnormalities of the brain	ENST00000349780	9	123.239.643	A>G	L571P	126	48	rs41296081	1082	12	0	1.054 / 121.408
ABCC8	ATP-binding cassette, sub-family C, member 8	#610374	AD	Transient neonatal diabetes mellitus type 2	Normal blood glucose levels	ENST00000389817	11	17.414.570	C>T	V1572I	164	55	rs8192690	1025	69	0	6.815 / 121.250
ETFA	Electron-transfer-flavo-protein, α-polypeptide	#231680	AR	Glutaric acidemia IIA	Normal excretion of organic acids in the urine	ENST00000559602	15	76.578.762	G>A	T67I	94	51	rs1801591	986	106	2	9.233 / 119.836
POLG	Polymerase (DNA directed), gamma	#613662	AD AR	Mitochondrial depletions syndrome type 4B	Absence of ophthalmoplegia, ptosis, or of Alpers syndrome	ENST00000268124	15	89.861.826	T>C	E1143G	95	47	rs2307441	1061	31	2	3.410 / 121.226
PMM2	Phosphomannomutase 2	#212065	AR	Congenital disorder of glycosylation type 1A	Absence of dysmorphic features or of assoicated symptoms seen in the various CDG syndromes	ENST00000539622	16	8.906.914	A>C	E114A	131	49	rs34258285	1068	26	0	2.343 / 121.412
PEX12	peroxisomal biogenesis factor 12	#614859	AR	Peroxysome biogenesis disorder type 3A	Absence of clinical features reminiscent of Zellweger syndrome	ENST00000225873	17	33.904.286	G>A	R151C	217	49	rs138731505	1093	1	0	251 / 120.956
TGIF1	TGFB-induced factor homeobox 1	#142946	AD	Holoprosencephaly type 4	Absence of structural abnormalities in the brain of the index patient	ENST00000330513	18	3.457.606	C>T	P292S	336	100	rs4468717	1010	82	2	73.106 / 121.356
CACNA1A	Calcium channel, voltage-dependent, P/Q type, alpha 1A subunit	#141500, #183086	AD	Familial hemiplegic migraine, Spinocerebellarataxis type 6	Absence of migraine, familial hemiplegic migraine or ataxia	ENST00000325084	19	13.409.407	C>T	E1015K	197	49	rs16024	1087	7	0	53 / 20.782
COL18A1	Collagen, type XVIII, alpha 1	#267750	AR	Knobloch syndrome	Absence of encephalocele, alopecia or of retinal degeneration	ENST00000400337	21	46.911.188	C>G	P706R	100	45	rs79980197	979	112	3	9.883 / 112.752
PRODH	Proline dehydrogenase (oxidase) 1	#239500	AR	Hyperprolinemia type I	Normal excretion of amino acids into the urine	ENST00000357068	22	18.905.934	A>G	L441P	48	52	rs2904551	1091	3	0	688 / 119.540
ARSA	Arylsulfatase A	#250100	AR	Metachromatic leukodystrophy	Absence of leukodystrophy on MRI	ENST00000395619	22	51.065.361	C>A	W195C	208	59	rs6151415	1050	42	2	6.348 / 118.420
KDM5C	Lysine (K)-specific demethylase 5C	#314690	XR	X-linked mental retardation	Absence of mental retardation	ENST00000375401	23	53.222.633	G>A	R1435C	315	50	rs140506776				107 / 87.472

Supplementary table 02: Variants causing an amino acid exchange within a panel of 343 genes associated with seizures that were predicted to be disease causing by the MutationTaster software: All variants only occurred heterozygously. Therefore diseases with autosomal recessive mode of inheritance could be ruled out. Other disorders could be excluded because the respective variant was present in the 1000 Genome project in heterozygous (HET) state or even homozygously for the minor allele or because additional symptoms characteristic for the respective disease were absent in the patient. **MOI,** mode of inheritance; **AR,** autosomal recessive; **AD**, autosomal dominant; **XR**, X-chromosomal recessive; **AAE,** amino acid exchange, ***** Frequencies refer to the genotypes of the 1000 Genome Project